Impaired local Vitamin D3 metabolism contributes to IL-36γ overproduction in epithelial cells in chronic rhinosinusitis with nasal polyps*

Qiao Xiao[1,2,3,#], Hai Wang[1,2,3,#], Jia Song[1,2,3], Zeng-Yin Qin[1,2,3], Li Pan[1,2,3], Bo Liao[1,2,3], Yi-Ke Deng[1,2,3], Jin Ma[1,2,3], Jin-Xin Liu[1,2,3], Jin Hu[1,2,3], Peisong Gao[4], Robert P. Schleimer[5,6], Zheng Liu[1,2,3]

[1] Department of Otolaryngology-Head and Neck Surgery, Tongji Hospital, Tongji Medical College, Huazhong University of Science and Technology, Wuhan, P.R. China

[2] Institute of Allergy and Clinical Immunology, Tongji Hospital, Tongji Medical College, Huazhong University of Science and Technology, Wuhan, P.R. China

[3] Hubei Clinical Research Center for Nasal Inflammatory Diseases, Wuhan, P.R. China

[4] Division of Allergy and Clinical Immunology, Johns Hopkins University School of Medicine, Baltimore, MD, USA

[5] Division of Allergy and Immunology, Department of Medicine, Northwestern University Feinberg School of Medicine, Chicago, IL, USA

[6] Department of Otolaryngology-Head and Neck Surgery, Northwestern University Feinberg School of Medicine, Chicago, IL, USA

[#] contributed equally

Rhinology 62: 2, 236 - 249, 2024
https://doi.org/10.4193/Rhin23.123

***Received for publication:**
April 9, 2023
Accepted: November 26, 2023

Abstract

Background: Vitamin D (VD) possesses immunomodulatory properties, but its role in chronic rhinosinusitis with nasal polyps (CRSwNP) remains poorly studied. Herein, we aim to explore the regulation and function of VD3 in CRSwNP.

Methods: 25-hydroxyvitamin D3 (25VD3) levels in serum and tissue lysates were detected by ELISA. The expression of VD receptor (VDR) and cytochrome P450 family 27 subfamily B member 1 (CYP27B1), the enzyme that converts 25VD3 to the active 1,25-hydroxyvitamin D3 (1,25VD3), and their expression regulation in human nasal epithelial cells (HNECs) were studied by RT-PCR, western blotting, immunofluorescence, and flow cytometry. RNA sequencing was performed to identify genes regulated by 1,25VD3 in HNECs. HNECs and polyp tissue explants were treated with 1,25VD3, 25VD3, and dexamethasone.

Results: 25VD3 levels in serum and nasal tissue lysates were decreased in patients with eosinophilic and noneosinophilic CRSwNP than control subjects. The expression of VDR and CYP27B1 were reduced in eosinophilic and noneosinophilic CRSwNP, particularly in nasal epithelial cells. VDR and CYP27B1 expression in HNECs were downregulated by interferon γ and poly (I:C). Polyp-derived epithelial cells demonstrated an impaired ability to convert 25VD3 to 1,25VD3 than control tissues. 1,25VD3 and 25VD3 suppressed IL-36γ production in HNECs and polyp tissues, and the effect of 25VD3 was abolished by siCYP27B1 treatment. Tissue 25VD3 levels negatively correlated with IL-36γ expression and neutrophilic inflammation in CRSwNP.

Conclusion: Reduced systemic 25VD3 level, local 1,25VD3 generation and VDR expression result in impaired VD3 signaling activation in nasal epithelial cells, thereby exaggerating IL-36γ production and neutrophilic inflammation in CRSwNP.

Key words: nasal polyps, cytochrome P450 family 27 subfamily B member 1, IL-36γ, neutrophilic inflammation, vitamin D receptor

Introduction

Chronic rhinosinusitis with nasal polyps (CRSwNP) represents an inflammatory disease characterized by exaggerated inflammation in sinonasal mucosa and polyp formation[1, 2]. It has become a widely prevalent health condition that imparts a substantial burden on individuals and society[1, 3]. CRSwNP is a heterogeneous disorder and typically characterized by type 2-dominated and eosinophilic inflammation, especially in the Western population[1]. Current treatment approaches for CRSwNP include medications involving nonspecific suppression of inflammation,

biologics, and endoscopic sinus surgery. Glucocorticoids and biologics targeting type 2 responses are effective in controlling eosinophilic inflammation in CRSwNP[1, 2]. However, more than half of CRSwNP patients in Asia does not present eosinophilic inflammation, but instead exhibits prominent neutrophil infiltration[4-8]. Intriguingly, CRSwNP in Caucasian patients, which is highly eosinophilic, also has significant levels of neutrophils[6, 9, 10]. Accumulating evidence has demonstrated the pathogenic role of neutrophils in CRSwNP[11]. For example, tissue neutrophils can elicit a plethora of cytokines and are associated with barrier function impairments and tissue remodeling in nasal polyps[9, 12]. More importantly, it has been demonstrated that tissue neutrophilia correlated with the severity of the disease, impaired response to oral corticosteroids, and even poor prognosis in patients with CRSwNP[10, 13]. Although excessive production of IL-8, G-CSF and IL-36γ has been linked with exaggerated neutrophilic inflammation in nasal polyps[6-8, 14], there is currently no available approach to directly target tissue neutrophilia as a treatment intervention.

Vitamin D3 (VD3) is a potent steroid hormone with immunomodulatory properties beyond its traditional role in calcium and phosphorus homeostasis[15-17]. VD3 has been reported to regulate the functions of a broad range of immune cells[16]. VD3 is obtained from nutrient sources or naturally synthesized in the skin[18]. It is metabolized to the primary circulating or storage form, 25-hydroxyvitamin D3 (25VD3), in the liver by 25-hydroxylase (cytochrome P450 family 2 subfamily R member 1, CYP2R1). 25VD3 is further converted to the active metabolite, 1,25-hydroxyvitamin D3 (1,25VD3), by the rate-limiting enzyme 1a-hydroxylase (cytochrome P450 family 27 subfamily B member 1, CYP27B1), which is expressed by renal epithelial cells[15, 16]. Nevertheless, emerging evidence has shown that respiratory epithelial cells, macrophages, T cells, and dendritic cells also express CYP27B1, indicating the extra-renal regulation of VD3 metabolism[16]. The biological activity of 1,25VD3 is mediated by the vitamin D receptor (VDR)[15, 19]. Upon binding ligand, cellular VDR dimerizes with the retinoic X receptor (RXR), translocates into the nucleus, and regulates expression of downstream genes through binding to the VD response elements in the promoter regions of target genes[15].

VD3 deficiency is associated with many chronic inflammatory diseases, including inflammatory bowel diseases, multiple sclerosis, asthma, and CRSwNP[20-23]. CYP27B1 and VDR expression have been reported in sinonasal mucosa[24]. However, local VD3 metabolism and the effects of VD3 signaling activation on sinonasal mucosal inflammation remain poorly understood. The present study aimed to explore 1) VD3 metabolism in the sinonasal mucosa in CRSwNP; 2) the regulation of CYP27B1 and VDR expression in CRSwNP; and 3) the effects of local VD3 signaling activation on sinonasal mucosal inflammation.

Materials and methods

Subjects and specimens

This study was approved by the Ethics Committee of Tongji Hospital and conducted with written informed consent from every patient. Seventy-five control subjects, 70 patients with eosinophilic CRSwNP and 67 patients with noneosinophilic CRSwNP were enrolled. The characteristics of subjects are provided in Table S1 in the Supplementary Materials. CRSwNP was classified as eosinophilic when the percent of tissue eosinophils exceeded 10% of total infiltrating cells[4, 7, 25, 26]. Control subjects were those undergoing septoplasty because of anatomic variations and without other sinonasal diseases. Inferior turbinate tissue and nasal polyp samples were taken from control subjects and CRSwNP patients during surgery, respectively. Human nasal epithelial cells (HNECs) were scraped from the middle meatus mucosa in control subjects and polyp tissues in CRSwNP patients, and subjected to cell culture experiments.

Histology and immunofluorescence staining

Hematoxylin and eosin, immunofluorescence staining with specific antibodies (Table S2 and Table S3 in the Supplementary Materials), and subsequent quantification were performed as previously described[4, 7, 27, 28].

Enzyme-linked immunosorbent assay (ELISA)

25VD3, 1,25VD3 and cytokines levels in serum, tissue homogenates, or cell culture supernatants were measured by using commercial ELISA kits[7]. The lower detection limits are listed in Table S4 in the Supplementary Materials.

Quantitative RT-PCR

Quantitative RT-PCR was performed with specific primers (Table S5 in the Supplementary Materials) as stated elsewhere[7, 28].

Western blotting

Western blotting was performed with specific antibodies (Table S6 in the Supplementary Materials) as previously reported[7, 28].

Dispersed nasal tissue cell preparation and flow cytometry

Tissue samples were dissociated mechanically[29]. Cell staining and flow cytometric analysis was performed as previously described[7, 28, 29].

Cell culture and treatment

Primary HNECs from control subjects were cultured using the air-liquid interface (ALI) method[30, 31], and treated with various CRS-associated cytokines, TLR agonists, 1,25VD3, or 25VD3. In some experiments, ALI-cultured HNECs were transfected with a small interfering RNA targeting CYP27B1 (siCYP27B1) before 25VD3 treatment[28].

When comparing the differences among the control, eosinophi-

lic CRSwNP, and noneosinophilic CRSwNP groups, HNECs were cultured submerged to retain the disease-specific expression pattern, which may represent CYP27B1 and VDR expression better than ALI-cultured HNECs in different study groups, and treated with 25VD3.

Promoter-luciferase reporter construct and luciferase assay

DNA fragments containing wild-type and mutated VDR binding sites of the *IL36G* promoter were generated by PCR and cloned into firefly luciferase reporter constructs. Submerged cultured HNECs from control subjects were transfected with the VDR overexpression plasmid and subsequently transfected with the indicated constructs together with the Renilla luciferase plasmid as previously reported[28].

Ex vivo polyp explant culture

Nasal polyp (NP) tissues were subjected to ex vivo ALI culture as previously described[25], and were stimulated with 1,25VD3, 25VD3 and dexamethasone for 24 or 48 hours.

RNA sequencing

Total RNA was extracted from HNECs stimulated with 1,25VD3 for 6 hours. Library construction and sequencing were performed by Annoroad Gene Technology (Beijing, China). All primary data have been uploaded to the Sequence Read Archive under accession number PRJNA889463.

Statistical analysis

Data derived from tissue studies were presented in dot plots with horizontal bars representing the medians and error bars showing interquartile ranges. Data distribution was evaluated by a Kolmogorov-Smirnov or Shapiro-Wilk test. For normally distributed data, an ANOVA with Tukey's post hoc test was applied to adjust for multiple comparisons, whereas an unpaired Student's t test was used for binary comparisons. For data not normally distributed, a Kruskal-Wallis test with the Dunn's post hoc test was adopted to adjust for multiple comparisons, and binary comparisons were assessed with a Mann-Whitney U 2-tailed test. Data derived from cell and tissue culture experiments were expressed as the mean and standard error of the mean (SEM) and analyzed by an unpaired Student's t test. For categorical variables, a chi-square test or Fisher's exact test was performed. Correlations were evaluated using Spearman's correlation. P value less than 0.05 was considered statistically significant.

More detailed information on the materials and methods is available in the Supplementary Materials.

Results

Decreased local CYP27B1 expression and 1,25VD3 generation in CRSwNP

To determine the association between VD3 and CRSwNP, we first measured 25VD3 levels in serum and nasal tissues. We found that serum 25VD3 levels were decreased in patients with CRSwNP, both eosinophilic and noneosinophilic type, compared with those in control subjects (Figure 1A). Interestingly, we observed a similar reduction in 25VD3 levels in NP tissues in both eosinophilic and noneosinophilic CRSwNP patients compared to control tissues, and no difference was discovered between eosinophilic and noneosinophilic patients (Figure 1A). The 25VD3 levels in nasal tissues positively correlated with those in serum (Figure 1B).

CYP27B1, the enzyme responsible for converting 25VD3 to the active 1,25VD3, was expressed in nasal tissues, and its expression was equally decreased in eosinophilic and noneosinophilic NPs in comparison with that in control tissues at both mRNA and protein levels (Figure 1C and D). To examine the tissue-specific cellular sources of CYP27B1, we performed immunofluorescence staining of sinonasal mucosal tissue sections and found that CYP27B1 was expressed by nasal epithelial cells as well as infiltrating immune cells in the lamina propria, including $CD3^+$ T cells, $CD11c^+$ dendritic cells, $CD20^+$ B cells, $CD68^+$ macrophages, myeloperoxidase $(MPO)^+$ neutrophils and $CD138^+$ plasma cells (Figure 1E and Figure S1). We also observed weak CYP27B1 expression in eosinophil peroxidase $(EPX)^+$ eosinophils and no expression in $tryptase^+$ mast cells (Figure S1). We further compared the expression intensity of CYP27B1 in epithelial cells and infiltrating immune cells by flow cytometric analysis of dispersed nasal tissue cells. We found that $CD45^-CD326^+$ epithelial cells had higher CYP27B1 expression than $CD45^+CD326^-$ hematopoietic cells and $CD45^-CD326^-$ stromal cells in nasal tissues from control subjects (Figure 1F). By immunofluorescence staining of tissue sections, we found that CYP27B1 immunoreactivity was significantly reduced in epithelium in CRSwNP compared with that in controls (Figure 1E). Consistently, flow cytometric analysis demonstrated lower fluorescence intensity of CYP27B1 in epithelial cells in both eosinophilic and noneosinophilic CRSwNP than that in controls (Figure 1G).

Given the significant expression of CYP27B1 by nasal epithelial cells, we tested if nasal epithelial cells were able to convert 25VD3 to 1,25VD3. We found that adding 25VD3 led to markedly increased levels of 1,25VD3 in supernatants of cultured HNECs from control subjects, which was significantly suppressed by knocking down CYP27B1 with siCYP27B1 (Figure 1H and Figure S2). Consistent with CYP27B1 expression levels, we discovered that after adding 25VD3, the levels of 1,25VD3 were lower in supernatants of HNECs derived from eosinophilic and noneosinophilic NPs than those in supernatants of HNECs obtained from control subjects (Figure 1I), suggesting an impairment of local generation of 1,25VD3 in patients with CRSwNP.

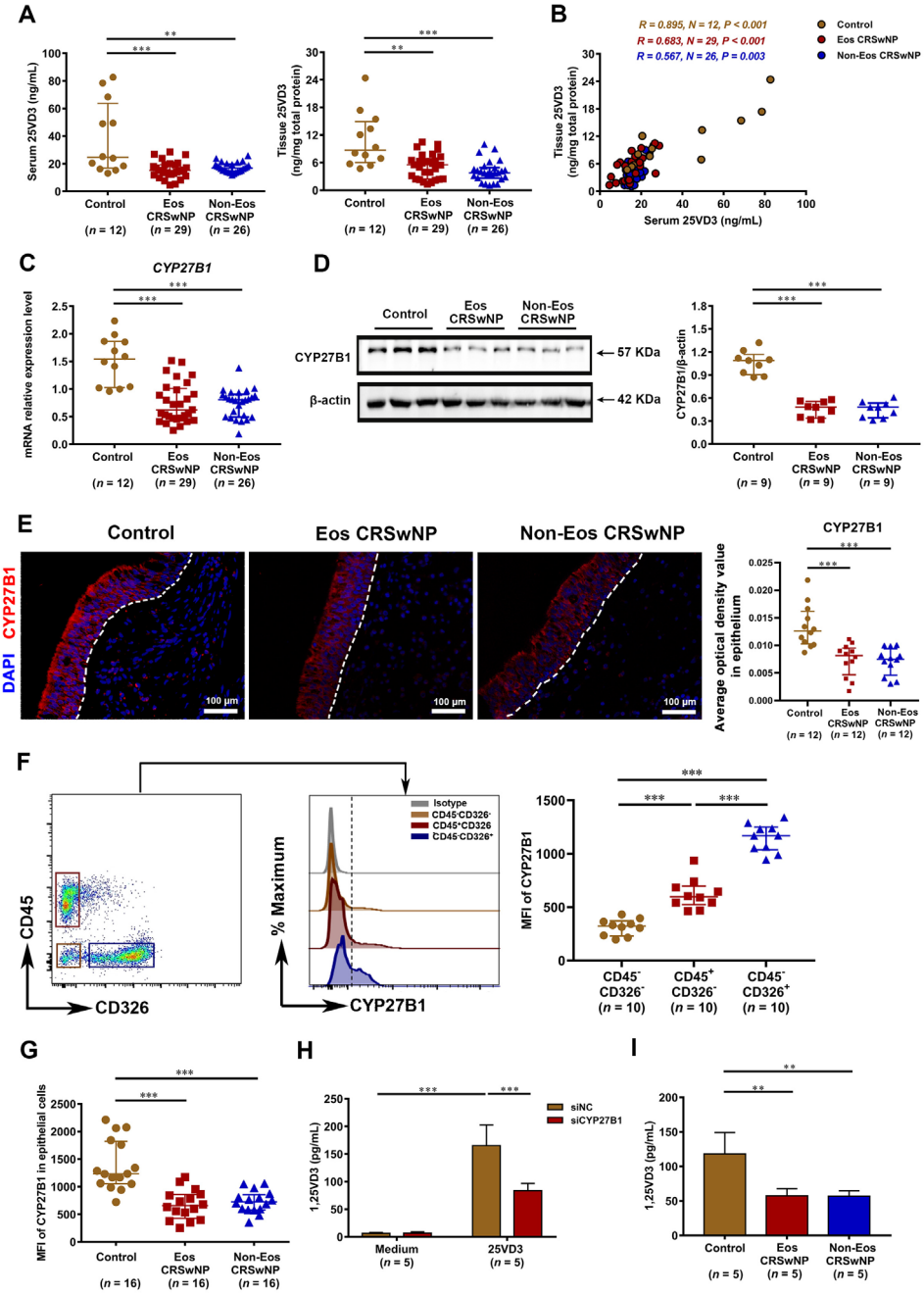

Figure 1. Decreased local CYP27B1 expression and 1,25VD3 generation in CRSwNP. (A) The 25VD3 levels in serum and nasal tissue lysates in different study groups as detected by ELISA. (B) Serum 25VD3 levels positively correlated with 25VD3 levels in nasal tissue lysates in different study groups. (C) and (D), The mRNA (C) and protein (D) levels of CYP27B1 in sinonasal mucosal samples in different study groups as detected by quantitative RT-PCR and western blotting, respectively. Representative western blots are shown. (E) Immunostaining of CYP27B1 in sinonasal mucosal tissues. Representative photomicrographs are shown (original magnification × 400). Scale bar, 100 μm. The dotted lines mark the basement membrane beneath the nasal epithelium. Fluorescence staining intensity in epithelium was quantified. (F) Dispersed nasal tissue cells from control subjects (n = 10) were subjected to flow cytometric analysis of CYP27B1 expression. Representative histogram of a control sample is shown, and the median fluorescence intensity (MFI) was quantified. (G) Flow cytometric analysis of the MFI of CYP27B1 in $CD45^{-}CD326^{+}$ epithelial cells in different study groups. (H) Human nasal epithelial cells (HNECs) obtained from control subjects were cultured with an air-liquid interface method. HNECs were transfected with siCYP27B1 or negative control siRNA (siNC) and treated with or without 25VD3 (n = 5). 1,25VD3 levels in cell culture supernatants were measured by ELISA. (I) HNECs scraped from different study groups were cultured submerged and treated with 25VD3 for 24 hours (n = 5 for each group). 1,25VD3 levels in culture supernatants were measured by ELISA. **P < 0.01 and ***P < 0.001. CRSwNP, chronic rhinosinusitis with nasal polyps; Eos, eosinophilic; Non-Eos, noneosinophilic.

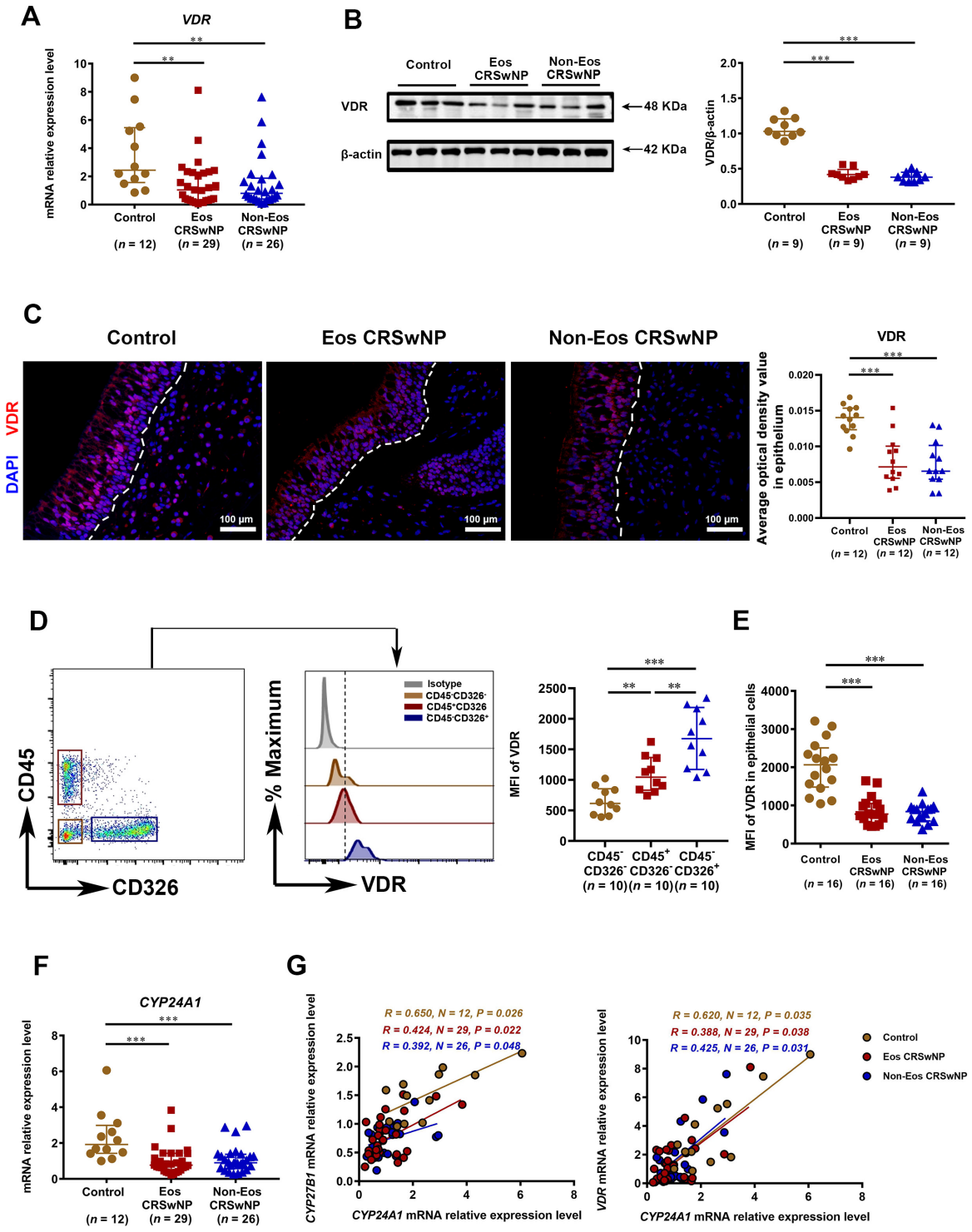

Figure 2. Decreased local VDR expression in CRSwNP. (A) and (B) VDR mRNA (A) and protein (B) levels in sinonasal mucosal samples in different study groups as detected by quantitative RT-PCR and western blotting, respectively. Representative western blots are shown. (C) Immunostaining of VDR in sinonasal mucosal tissues. Representative photomicrographs are shown (original magnification × 400). Scale bar, 100 μm. The dotted lines mark the basement membrane beneath the nasal epithelium. Fluorescence staining intensity in epithelium was quantified. (D) Dispersed nasal tissue cells from control subjects (n = 10) were subjected to flow cytometric analysis of VDR expression. Representative histogram of a control sample is shown, and the median fluorescence intensity (MFI) was quantified. (E) Flow cytometric analysis of the MFI of VDR in $CD45^{-}CD326^{+}$ epithelial cells in different study groups. (F) The mRNA expression level of *CYP24A1* in sinonasal mucosal samples in different study groups as detected by RT-PCR. (G) Tissue *CYP24A1* mRNA expression positively correlated with tissue *CYP27B1* and tissue *VDR* mRNA expression in different study groups. **P < 0.01 and ***P < 0.001. CRSwNP, chronic rhinosinusitis with nasal polyps; Eos, eosinophilic; Non-Eos, noneosinophilic.

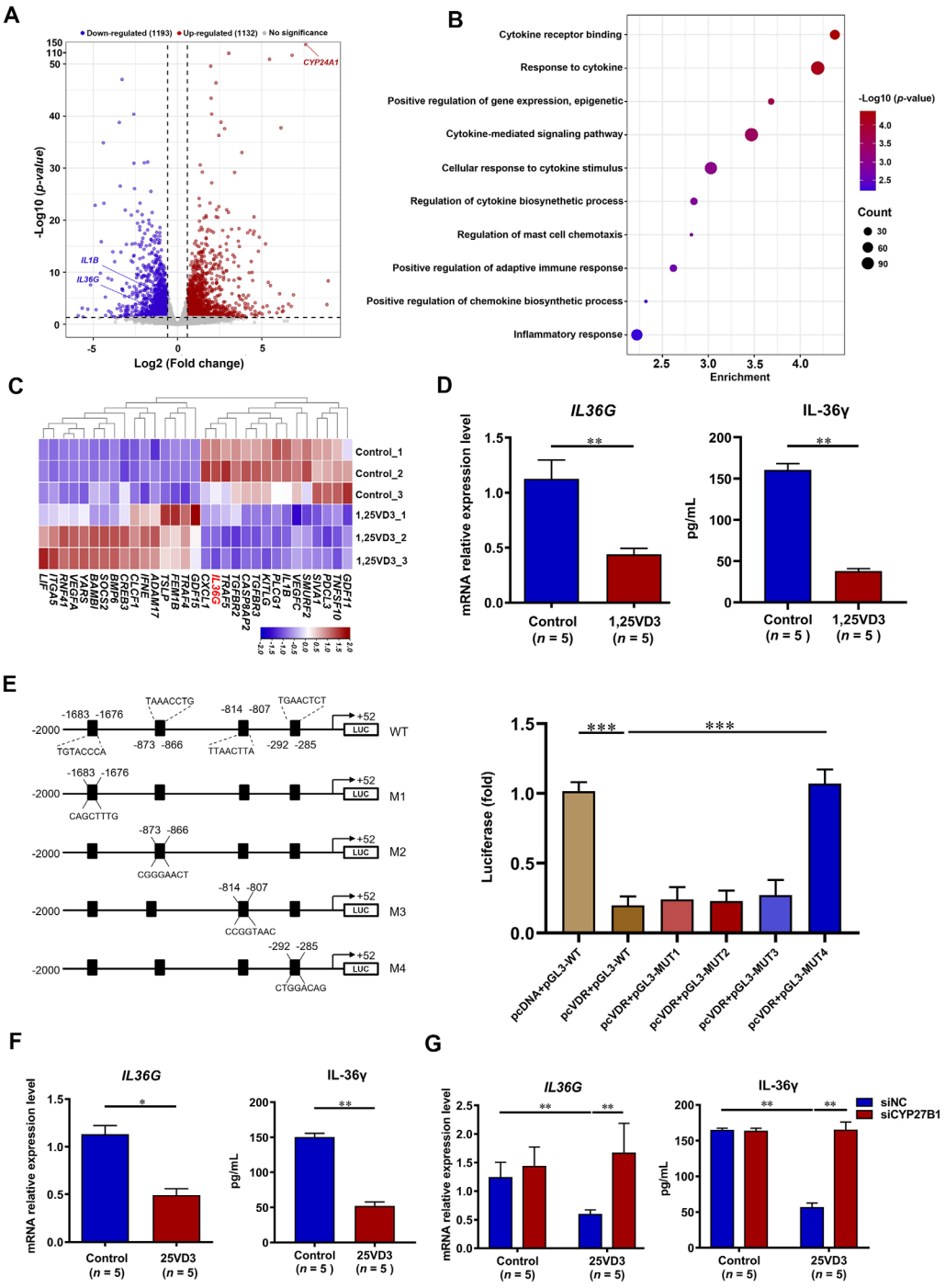

Figure 3. 1,25VD3 and 25VD3 downregulate IL-36γ production in nasal epithelial cells. Human nasal epithelial cells (HNECs) scraped from control subjects were cultured with an air-liquid interface (ALI) method. (A) HNECs (n = 3) were treated with 1,25VD3 for 6 hours. Cells were harvested for RNA sequencing. Volcano Plot map shows 1,132 up-regulated and 1,193 down-regulated genes altered by 1,25VD3 in HNECs. (B) GO enrichment analysis of differentially expressed genes. (C) Heatmap shows differentially expressed genes involved in the cytokine receptor binding pathway. (D) HNECs were stimulated with 1,25VD3, and IL-36γ mRNA levels in HNECs and protein levels in culture supernatants were detected by RT-PCR (n = 5) and ELISA (n = 5), respectively. (E) Left panel, a schematic presentation of four putative VDR binding sites and their mutants in IL36G promoter. Right panel, HNECs were cultured submerged and transfected with VDR overexpression or control plasmid and indicated constructs. Twenty-four hours later, cell lysates were harvested for luciferase assay (n = 6). (F) HNECs were stimulated with 25VD3. *IL-36γ* mRNA levels in HNECs and protein levels in culture supernatants were detected by RT-PCR (n = 5) and ELISA (n = 5), respectively. (G) HNECs were treated with siRNA targeting CYP27B1 and 25VD3. IL-36γ mRNA expression level in HNECs and protein levels in culture supernatants were detected by RT-PCR (n = 5) and ELISA (n = 5), respectively. *P < 0.05, **P < 0.01 and ***P < 0.001, compared with controls.

Decreased local VDR expression in CRSwNP

The biological activity of VD is mediated by the nuclear hormone receptor, VDR[15, 32]. We found that the mRNA and protein levels of VDR were decreased comparably in eosinophilic and noneosinophilic NPs compared with those in control tissues (Figure 2A and B). Immunofluorescence staining of tissue sections revealed immunoreactivity of VDR in nasal epithelial cells and infiltrating cells in the lamina propria, including $CD3^+$ T cells, $CD11c^+$ dendritic cells, $CD20^+$ B cells, $CD68^+$ macrophages, MPO^+ neutrophils, and $CD138^+$ plasma cells in sinonasal tissues (Figure 2C and Figure S3). We also observed weak VDR expression in EPX^+ eosinophils and $tryptase^+$ mast cells (Figure S3). We further compared the expression intensity of VDR in epithelial cells and infiltrating immune cells by flow cytometric analysis of dispersed nasal tissue cells. We found that $CD45^-CD326^+$ epithelial cells had higher VDR expression levels than those in $CD45^+CD326^-$ hematopoietic cells and $CD45^-CD326^-$ stromal cells in nasal tissues from control subjects (Figure 2D). Immunofluorescence staining of tissue sections revealed that VDR immunoreactivity was significantly lower in epithelium in CRSwNP than that in controls (Figure 2C). Consistently, flow cytometric analysis demonstrated decreased fluorescence intensity of VDR in nasal epithelial cells in both eosinophilic and noneosinophilic CRSwNP compared to that in control tissues (Figure 2E).

The reduced ability to generate 1,25VD3 locally and lower VDR expression may lead to impaired VD3 signaling activation in CRSwNP. To test this possibility, we examined the expression of cytochrome P450 family 24 subfamily A member 1 (CYP24A1), which is a well-known VD3 signaling induced gene. We found that the mRNA expression of *CYP24A1* was significantly downregulated in eosinophilic and noneosinophilic NPs in comparison with control tissues (Figure 2F). In addition, *CYP24A1* mRNA expression positively correlated with *CYP27B1* and *VDR* mRNA expression in sinonasal tissues (Figure 2G).

1,25VD3 downregulates IL-36γ production in HNECs

To dissect the effects of VD3 signaling activation on the function of nasal epithelial cells, HNECs obtained from control subjects were treated with 1,25VD3 and subjected to subsequent RNA sequencing. We identified 1,132 upregulated genes and 1,193 downregulated genes in HNECs upon 1,25VD3 treatment, including upregulated *CYP24A1* (Figure 3A). Gene ontology-enrichment analysis showed that these differentially expressed genes were involved in a wide range of inflammatory processes, such as cytokine receptor binding, response to cytokine, and cytokine-mediated signaling pathway, etc. (Figure 3B).

In the first ranked inflammation relevant pathway, cytokine receptor binding, there were 15 downregulated and 16 upregulated genes (Figure 3C). Among them, *IL36G* is of great interest to us. Our previous study suggested that IL-36γ may play a crucial role in aggravating neutrophilic inflammation in CRSwNP[7].

Neutrophils have been reported to associate with poor outcomes after oral corticosteroid treatment and endoscopic sinus surgery[9-13]. In line with previous reports[7], we found that the number of MPO^+ neutrophils as well as IL-36γ mRNA and protein levels were higher in both eosinophilic and noneosinophilic NPs than those in control tissues (Figure S4A and B). By performing additional cell culture experiments with HNECs obtained from control subjects, we observed an inhibitory effect of 1,25VD3 on IL-36γ production in HNECs at both mRNA and protein levels (Figure 3D).

To further investigate the mechanism underlying the downregulation of IL-36γ by 1,25VD3, we determined whether the expression of *IL36G* could be directly trans-regulated by VDR. We inspected the promoter sequence of *IL36G* and identified four putative VDR binding sites (-1683 to -1676, -873 to -866, -814 to -807, and -292 to -285 relative to the transcriptional start site) using the JASPAR database (http://jaspar.binf.ku.dk/) (Figure 3E). We subsequently examined the binding of VDR to these sites using a luciferase reporter assay. We found that luciferase activity was significantly reduced in HNECs transfected with a plasmid containing the wild-type *IL36G* promoter sequence upon overexpression of VDR with a VDR plasmid (pcVDR) (Figure 3E and Figure S5). The inhibitory effect of pcVDR was abolished only when the fourth VDR binding site (-292 to -285) in the promoter of *IL36G* was mutated (Figure 3E). Our results suggest that direct binding of VDR to the *IL36G* promoter mediates a transcriptional regulation of expression of *IL36G*.

Interestingly, we observed that 25VD3 mimicked the suppressive effect of 1,25VD3 on IL-36γ production in HNECs (Figure 3F), and this effect was abolished when CYP27B1 was knocked down (Figure 3G), reinforcing the importance of local metabolism and activation of VD3 in exerting its regulatory function. Our previous study discovered that IL-36γ production in HNECs could be upregulated by poly (I:C), IL-1β, TNF-α, and IL-17A[7]. In the present study, we reported that 1,25VD3 and 25VD3 were able to inhibit IL-36γ production induced by poly (I:C), IL-1β, TNF-α and IL-17A in HNECs (Figure S6A-D).

1,25VD3 downregulates IL-36γ production in NP explants

We further tested the effect of VD3 in comparison with glucocorticoids on tissue inflammation pattern in patients with CRSwNP. NP explants from both eosinophilic (Figure 4A and B) and noneosinophilic CRSwNP patients (Figure 4C and D) were cultured ex vivo and treated with 1,25VD3, 25VD3 or dexamethasone. Interestingly, we found that IL-36γ and IL-17A production were downregulated by 1,25VD3 and 25VD3, but not dexamethasone, in both eosinophilic and noneosinophilic NP explants (Figure 4). In contrast, IL-5 production was downregulated by dexamethasone, but not by 1,25VD3 or 25VD3 (Figure 4). Expression of interferon γ (IFN-γ) was downregulated by both VD3 and dexamethasone in eosinophilic and noneosinophilic

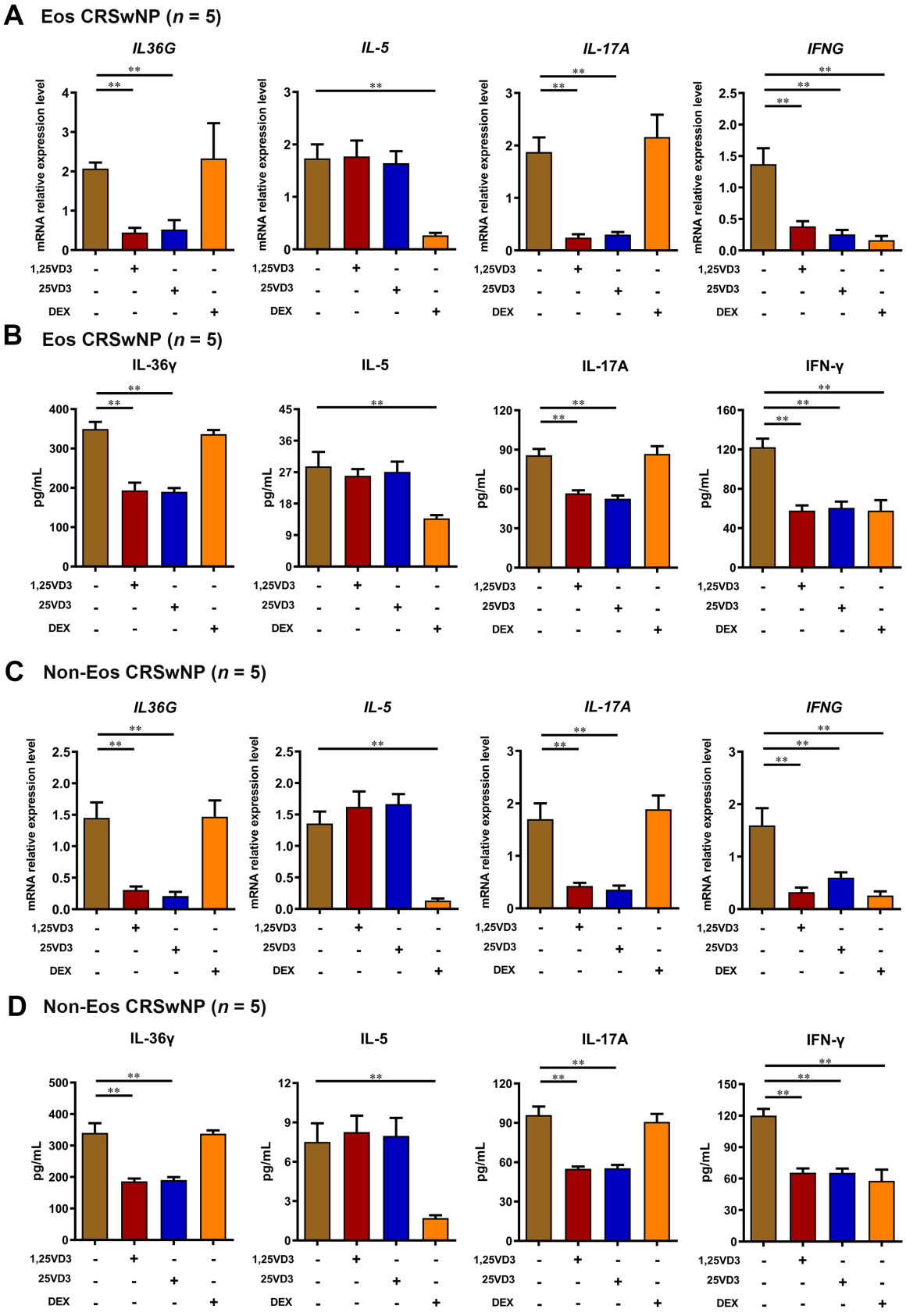

Figure 4. 1,25VD3 downregulates IL-36γ production in NP explants. NP explants were cultured ex vivo and treated with 1,25VD3, 25VD3, or dexamethasone. The mRNA expression levels of cytokines in eosinophilic NPs (A) and noneosinophilic NPs (C) were detected by RT-PCR (n = 5 for each group). The protein levels of cytokines in culture supernatant of eosinophilic NPs (B) and noneosinophilic NPs (D) were detected by ELISA (n = 5 for each group). **P < 0.01. CRSwNP, chronic rhinosinusitis with nasal polyps; Eos, eosinophilic; Non-Eos, noneosinophilic.

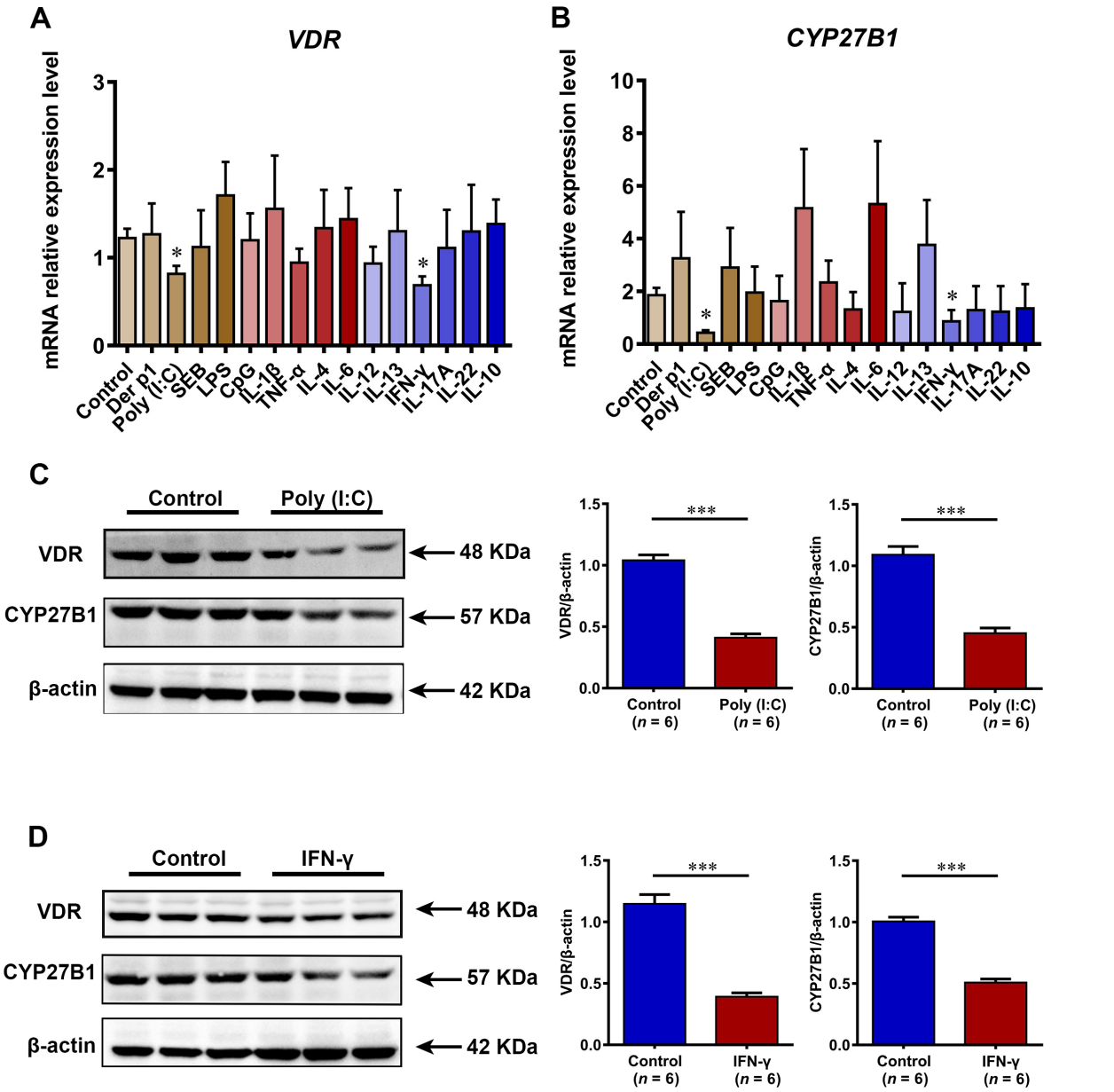

Figure 5. Regulation of VDR and CYP27B1 expression in nasal epithelial cells. Human nasal epithelial cells (HNECs) scraped from control subjects were cultured with an air-liquid interface method. (A) and (B), HNECs were treated with various CRS-associated cytokines and TLR agonists for 6 hours. After stimulation, cells were harvested for quantitative RT-PCR assay (n = 5). (C) and (D), HNECs were stimulated with poly (I:C) (C) or IFN-γ (D) for 24 hours. After stimulation, cells were harvested for western blotting (n = 6). Representative blots are shown. *P < 0.05 and ***P < 0.001, compared with controls.

NP explants (Figure 4). The changes of IL-36γ, IL-5, IL-17A and IFN-γ after treatment were consistent at mRNA (Figure 4A and C) and protein levels (Figure 4B and D).

Regulation of VDR and CYP27B1 expression in HNECs.

To gain insight into the mechanism underlying decreased VDR and CYP27B1 expression in CRSwNP, we explored the regulation of VDR and CYP27B1 expression in HNECs by allergens, TLR agonists, and cytokines that have been associated with CRSwNP pathogenesis[27, 28]. We found that the mRNA expression of *VDR* and *CYP27B1* in HNECs were significantly downregulated by IFN-γ and poly (I:C) (Figure 5A and B). No significant effect was observed for Der p1, staphylococcal enterotoxin B (SEB), lipopolysaccharide (LPS), CpG, IL-1β, TNF-α, IL-4, IL-6, IL-12, IL-13, IL-17A, IL-22 and IL-10 (Figure 5A and B). The downregulation of VDR and CYP27B1 by IFN-γ and poly (I:C) was confirmed at protein levels (Figure 5C and D).

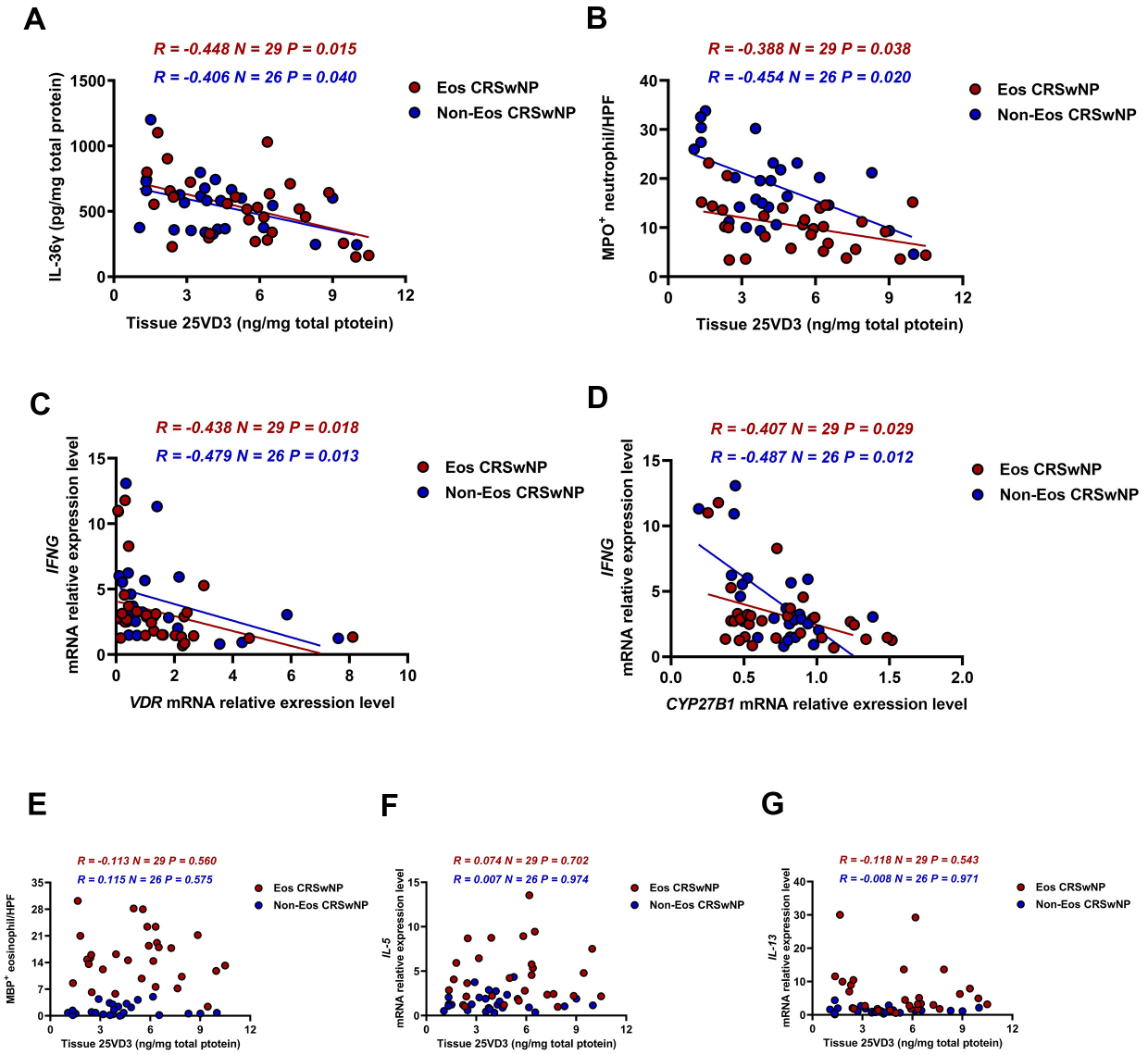

Figure 6. Tissue 25VD3 levels correlate with neutrophilic inflammation in CRSwNP. (A) and (B), Tissue 25VD3 levels positively correlated with IL-36γ protein levels (A) and the number of myeloperoxidase (MPO)$^+$ neutrophils (B) in patients with CRSwNP. (C) and (D), Tissue *VDR* (C) and *CYP27B1* (D) mRNA expression negatively correlated with tissue *IFNG* mRNA expression in patients with CRSwNP. (E-G) No correlation of tissue 25VD3 levels with the number of major basic protein (MBP)$^+$ eosinophils (E), or tissue *IL-5* (F) or *IL-13* (G) mRNA levels in patients with CRSwNP. CRSwNP, chronic rhinosinusitis with nasal polyps; Eos, eosinophilic; Non-Eos, noneosinophilic.

Tissue 25VD3 levels correlate with neutrophilic inflammation in CRSwNP

Last, we studied whether the in vitro mechanisms could be recapitulated in vivo by studying patient samples ex vivo. We found negative correlations of tissue 25VD3 levels with IL-36γ levels and the number of MPO$^+$ neutrophils in patients with eosinophilic and noneosinophilic CRSwNP (Figure 6A and B). In addition, tissue *VDR* and *CYP27B1* mRNA expression negatively correlated with tissue *IFNG* mRNA expression in CRSwNP (Figure 6C and D). We failed to find any association between tissue 25VD3 levels and the number of major basic protein (MBP)$^+$eosinophils, tissue *IL-5* or *IL-13* mRNA expression in CRSwNP (Figure 6E-G).

Discussion

In this study, we revealed that the reduced systemic 25VD3 levels, impaired local 1,25VD3 generation due to CYP27B1 deficiency, and decreased VDR expression collectively result in weakened VD3 signaling activation in nasal epithelial cells, thereby exaggerating IL-36γ production and neutrophilic inflammation in CRSwNP. VD3 may hold therapeutic potential for suppressing neutrophilic inflammation in CRSwNP.

The half-life for 1,25VD3 is only 4-6 hours, in contrast to the 3-week half-life of 25VD3. Thus, 25VD3 is thought to represent the systemic reservoir of VD3[33]. In accordance with the previous study by Mulligan et al.[24], we found a systemic 25VD3 deficien-

cy in eosinophilic and noneosinophilic CRSwNP patients. VD3 is obtained through dietary intake or synthesized by the skin after sunshine exposure, and further converted to 25VD3 by CYP2R1 in the liver[17]. The systemic deficiency in 25VD3 in CRSwNP patients is possibly related to reduced VD3 intake, decreased sunlight exposure, or impaired VD3 metabolism in liver. Mulligan et al. showed that a VD3 deficient diet led to decreased systemic 25VD3 levels in a mouse model of *Aspergillus fumigatus*-induced CRS[34]. However, there is still lack of direct epidemiological evidence to support those associations in CRSwNP patients. Moreover, we found that tissue 25VD3 levels were also decreased in eosinophilic and noneosinophilic CRSwNP patients, and positively correlated with serum 25VD3 levels. It suggests that the 25VD3 levels in nasal tissues may be primarily determined by its systemic levels, consistent with the previous report[24].

CYP27B1 is essential for the metabolism of 25VD3 to 1,25VD3[16]. CYP27B1 is typically expressed by renal epithelial cells, and can be regulated by circulating calcium, parathyroid hormone and fibroblast growth factor-23 (FGF-23)[17, 35]. Mostafa et al. found no significant difference in serum calcium levels between CRSwNP and control group[36]. In addition, there is no evidence showing parathyroid dysfunction or abnormal FGF-23 levels in CRSwNP patients. We expect that the deficiency of 25VD3 may lead to a subsequent reduction of 1,25VD3 systemically in patients with CRSwNP. However, well-controlled sample collection and timely measurement will be needed to test this hypothesis. Extra-renal expression of CYP27B1 has been demonstrated in respiratory epithelial cells, macrophages, T cells, and dendritic cells[17]. In this study, we found significantly reduced CYP27B1 expression, particularly in nasal epithelial cells in both CRSwNP subtype compared with controls. This reduction likely leads to observed impaired capacity of nasal epithelial cells to convert 25VD3 to 1,25VD3 in eosinophilic and noneosinophilic CRSwNP patients. Taken together, both local 25VD3 deficiency and 1,25VD3 synthesis impairment may result in the loss of VD3-mediated regulatory function on nasal mucosa.

After binding to VDR, the 1,25VD3/VDR/RXR complex translocates into the nucleus, and regulates downstream gene expression. The nuclear localization of VDR indicates an activation of VD signaling pathway. Consistent with the previous study[37], our immunofluorescence staining showed the nuclear localization of VDR in sinonasal mucosa and VDR expression was reduced in eosinophilic and noneosinophilic CRSwNP, particularly in nasal epithelial cells. The decreased VDR expression would further blunt VD3 effect in CRSwNP, which was supported by the downregulation of *CYP24A1*, a classical gene regulated by VD3 signaling, in NPs[16, 38]. Furthermore, we compared the mRNA expression of *VDR* and *CYP27B1* in control ethmoid sinus mucosa and control inferior turbinate tissues, and found no significant difference (data not shown). It suggests that dysregulated local VD3 signaling may be specific for NPs, but not due to the origin of tissues.

Although immunomodulatory effects of VD on $CD4^+$ T cells[39], $CD8^+$ T cells[40], macrophage[41], and B cells[42] have been reported, the investigations of VD3 effects on airway epithelial cells remain limited. Here, we identified 2,325 genes significantly regulated by 1,25VD3 in nasal epithelial cells. Among them, the reduction of *IL1*β and upregulation of *CYP24A1* upon 1,25VD3 treatment have previously been reported in macrophages and renal epithelial cells[15, 43, 44], respectively. In this study, we found that activation of VD3 signaling significantly suppressed IL-36γ production in nasal epithelial cells. Previously, Beatriz et al. discovered an inhibitory effect of VD3 on IL-36γ production in keratinocytes in a psoriasis mouse model[45]. IL-36γ has been reported to play a role in the initiation and maintenance of neutrophilic inflammation in CRSwNP[7]. In this study, we provided several lines of evidence for a regulatory effect of VD3 on IL-36γ production and neutrophilic inflammation in CRSwNP: 1) 1,25VD3 was able to suppress IL-36γ production in nasal epithelial cells not only at baseline but also under induction by poly (I:C), IL-17A, IL-1β, and TNF-α; 2) Bioinformatics analysis and luciferase reporter assay demonstrated that *IL36G* was transregulated by VDR; 3) The suppressive effect of 25VD3 on IL-36γ production was dependent on CYP27B1; 4) Tissue 25VD3 levels negatively correlated with IL-36γ levels and MPO^+ neutrophil numbers in NPs. Notably, we observed a comparable reduction in VD3 signaling in both CRSwNP subtypes, although noneosinophilic CRSwNP demonstrated higher numbers of neutrophils than eosinophilic CRSwNP. It indicates that VD3 may be not the sole driver of neutrophilia in CRSwNP. Other factors promoting or inhibiting neutrophil infiltration in eosinophilic and noneosinophilic CRSwNP deserve further studies.

To investigate the therapeutic potential of VD3 on CRSwNP, we treated NP explants with 1,25VD3 and 25VD3 in comparison with dexamethasone. We found that 25VD3 and 1,25VD3 treatment significantly attenuated IL-17A and IFN-γ expression in NPs. VD3 has previously been shown to directly inhibit the differentiation and activation of Th17 and Th1 cells, but not Th2 cells, and thus lead to reduced production of IL-17A and IFN-γ[16, 46]. We have recently shown that neutrophils were also an important source of IL-17A and IFN-γ in CRSwNP[7, 47]. Downregulation of IL-36γ by VD3 may suppress neutrophil activation and thus reduce IL-17A and IFN-γ production in NPs. In this study, we found that VDR was also expressed by neutrophils in NPs. Whether VD3 has a direct effect on neutrophils deserves further studies.

Remarkably, we found distinct effect of VD3 and dexamethasone on IL-36γ and IL-5 production in NP explants. Glucocorticoids stand as major anti-inflammatory treatment for CRSwNP and are effective to control type 2 and eosinophilic inflammation in CRSwNP[1]. Nevertheless, Wen et al. found that oral prednisone failed to suppress neutrophilic inflammation in Chinese CRSwNP patients[13]. Wang et al. discovered that dexamethasone was una-

ble to suppress IL-36γ-induced neutrophil activation in NPs[7]. By extending those findings, we demonstrated that dexamethasone did not suppress IL-36γ production in NPs although it significantly inhibited IL-5 production. On the contrary, we found that the 1,25VD3 or 25VD3 had no effect on IL-5 production and there were no associations between 25VD3 levels and eosinophil numbers, IL-5, or IL-13 levels in NPs, suggesting that VD3 may have no significant effect on type 2 and eosinophilic inflammation in CRSwNP. Our results indicate a complementary role of glucocorticoids and VD3 in relieving eosinophilic and neutrophilic inflammation in CRSwNP. Several studies have reported that VDR was expressed in lower airways[48, 49], and its expression was decreased in pediatric asthmatic patients[50, 51]. In addition, IL-36γ levels were found to be increased in bronchoalveolar lavage fluid of patients with neutrophilic asthma[52]. Therefore, it is possible to extrapolate our outcomes to other type 2-inflammation mediated airway diseases which are mixed with neutrophilic inflammation. However, further studies are warranted to support this notion.

After screening various cytokines and TLR ligands associated with CRSwNP, we found that CYP27B1 and VDR expression in nasal epithelial cells were downregulated by poly (I:C) and IFN-γ. Elevated IFN-γ expression has been shown in both eosinophilic and noneosinophilic NPs[4, 7]. We discovered negative correlations of *IFNG* mRNA expression with *CYP27B1* and *VDR* mRNA expression in NPs. Thus, decreased *CYP27B1* and *VDR* expression in nasal epithelial cells in CRSwNP may result from, at least in part, the local inflammatory milieu. In contrast to the finding in macrophages, we found that LPS had no significant effect on *CYP27B1* expression in HNECs, indicating a cell-context dependent regulation of *CYP27B1* expression.

Heretofore, three single-center clinical trials have been conducted to explore the effects of VD3 supplement on patients with CRS. VD3 supplement has been found to reduce the severity of symptoms and NP recurrence after surgery in CRS patients significantly[54-56]. However, those studies are limited by small sample size, short treatment duration, and lack of serum VD3 level monitoring. Moreover, there is no study exploring the effect of VD3 supplement on CRS with different inflammation patterns. It is will be interesting to investigate the effect of VD3 supplement on CRS with distinct endotypes by well-designed and controlled clinical trials in future, which may aid in personalized medicine for CRS.

Our study has several limitations. Immunomodulatory effects of VD3 have only been investigated in nasal epithelial cells. The effects of VD3 on infiltrating immune cells with VDR expression in the context of CRSwNP remain to be determined. In addition, the lack of a validated murine CRSwNP model with predominant neutrophilic inflammation hinders mechanistic study of our findings in vivo.

Conclusion

Our study indicates that reduction in systemic 25VD3 levels, local 1,25VD3 generation, and VDR expression may collectively lead to impaired VD3 signaling activation and subsequent exaggerated IL-36γ production and neutrophilic inflammation in CRSwNP. Our findings provide new insights into the VD3 treatment on CRSwNP, focusing on neutrophilic inflammation.

Authorship contribution

QX and HW performed histology and immunofluorescence staining, cell culture, ELISA, flow cytometry, western blotting, and ex vivo polyp explant culture experiments, analyzed data, and prepared the manuscript. JS and ZYQ performed immunofluorescence staining experiments. LP and BL performed RT-PCR. YKD, JM, JXL, and JH participated in tissue sample collection and data discussion. RPS and PG participated in data discussion and manuscript preparation. ZL designed the study and prepared the manuscript.

Funding

This study was supported by the National Key Research and Development Program of China (2022YFE0131200, ZL), and the National Natural Science Foundation of China (NSFC) grants 81920108011 and 82130030 (ZL), 82000965 (HW), and 81900925 (JS).

Conflict of interest

The authors have no competing interests to declare.

References

1. Fokkens WJ, Lund VJ, Hopkins C, Hellings PW, Kern R, Reitsma S, et al. European Position Paper on Rhinosinusitis and Nasal Polyps 2020. Rhinology. 2020;58(Suppl S29):1-464.
2. Orlandi RR, Kingdom TT, Smith TL, Bleier B, DeConde A, Luong AU, et al. International consensus statement on allergy and rhinology: rhinosinusitis 2021. Int Forum Allergy Rhinol. 2021;11(3):213-739.
3. Schleimer RP. Immunopathogenesis of chronic rhinosinusitis and nasal polyposis. Annu Rev Pathol. 2017;12:331-57.
4. Cao PP, Li HB, Wang BF, Wang SB, You XJ, Cui YH, et al. Distinct immunopathologic characteristics of various types of chronic rhinosinusitis in adult Chinese. J Allergy Clin Immunol. 2009;124(3):478-84, 84 e1-2.
5. Van Bruaene N, Perez-Novo CA, Basinski TM, Van Zele T, Holtappels G, De Ruyck N, et al. T-cell regulation in chronic paranasal sinus disease. J Allergy Clin Immunol. 2008;121(6):1435-41, 41 e1-3.
6. Van Zele T, Claeys S, Gevaert P, Van Maele G, Holtappels G, Van Cauwenberge P, et al. Differentiation of chronic sinus diseases by measurement of inflammatory mediators. Allergy. 2006;61(11):1280-9.
7. Wang H, Li ZY, Jiang WX, Liao B, Zhai GT, Wang N, et al. The activation and function of IL-36gamma in neutrophilic inflammation in chronic rhinosinusitis. J Allergy Clin Immunol. 2018;141(5):1646-58.
8. Wang X, Zhang N, Bo M, Holtappels G, Zheng M, Lou H, et al. Diversity of T(H)

cytokine profiles in patients with chronic rhinosinusitis: A multicenter study in Europe, Asia, and Oceania. J Allergy Clin Immunol. 2016;138(5):1344-53.
9. Pothoven KL, Norton JE, Suh LA, Carter RG, Harris KE, Biyasheva A, et al. Neutrophils are a major source of the epithelial barrier disrupting cytokine oncostatin M in patients with mucosal airways disease. J Allergy Clin Immunol. 2017;139(6):1966-78 e9.
10. Liao B, Liu JX, Li ZY, Zhen Z, Cao PP, Yao Y, et al. Multidimensional endotypes of chronic rhinosinusitis and their association with treatment outcomes. Allergy. 2018;73(7):1459-69.
11. Wang H, Pan L, Liu Z. Neutrophils as a protagonist and target in chronic rhinosinusitis. Clin Exp Otorhinolaryngol. 2019;12(4):337-47.
12. Shi LL, Xiong P, Zhang L, Cao PP, Liao B, Lu X, et al. Features of airway remodeling in different types of Chinese chronic rhinosinusitis are associated with inflammation patterns. Allergy. 2013;68(1):101-9.
13. Wen W, Liu W, Zhang L, Bai J, Fan Y, Xia W, et al. Increased neutrophilia in nasal polyps reduces the response to oral corticosteroid therapy. J Allergy Clin Immunol. 2012;129(6):1522-8 e5.
14. Ruan JW, Zhao JF, Li XL, Liao B, Pan L, Zhu KZ, et al. Characterizing the neutrophilic inflammation in chronic rhinosinusitis with nasal polyps. Front Cell Dev Biol. 2021;9:793073.
15. Christakos S, Dhawan P, Verstuyf A, Verlinden L, Carmeliet G. Vitamin D: metabolism, molecular mechanism of action, and pleiotropic effects. Physiol Rev. 2016;96(1):365-408.
16. Sassi F, Tamone C, D'Amelio P. Vitamin D: nutrient, hormone, and immunomodulator. nutrients. 2018;10(11).
17. Wei R, Christakos S. Mechanisms underlying the regulation of innate and adaptive immunity by vitamin D. Nutrients. 2015;7(10):8251-60.
18. Bozzetto S, Carraro S, Giordano G, Boner A, Baraldi E. Asthma, allergy and respiratory infections: the vitamin D hypothesis. Allergy. 2012;67(1):10-7.
19. Haussler MR, Whitfield GK, Haussler CA, Hsieh JC, Thompson PD, Selznick SH, et al. The nuclear vitamin D receptor: biological and molecular regulatory properties revealed. J Bone Miner Res. 1998;13(3):325-49.
20. Wu Z, Liu D, Deng F. The role of vitamin D in immune system and inflammatory bowel disease. J Inflamm Res. 2022;15:3167-85.
21. Yeh WZ, Gresle M, Jokubaitis V, Stankovich J, van der Walt A, Butzkueven H. Immunoregulatory effects and therapeutic potential of vitamin D in multiple sclerosis. Br J Pharmacol. 2020;177(18):4113-33.
22. Poon AH, Mahboub B, Hamid Q. Vitamin D deficiency and severe asthma. Pharmacol Ther. 2013;140(2):148-55.
23. Shahangian A, Schlosser RJ. Role of Vitamin D in Pathogenesis of Chronic Sinusitis with Nasal Polyposis. Adv Otorhinolaryngol. 2016;79:86-90.
24. Mulligan JK, Nagel W, O'Connell BP, Wentzel J, Atkinson C, Schlosser RJ. Cigarette smoke exposure is associated with vitamin D3 deficiencies in patients with chronic rhinosinusitis. J Allergy Clin Immunol. 2014;134(2):342-9.
25. Song J, Wang H, Zhang YN, Cao PP, Liao B, Wang ZZ, et al. Ectopic lymphoid tissues support local immunoglobulin production in patients with chronic rhinosinusitis with nasal polyps. J Allergy Clin Immunol. 2018;141(3):927-37.
26. Zhai GT, Wang H, Li JX, Cao PP, Jiang WX, Song J, et al. IgD-activated mast cells induce IgE synthesis in B cells in nasal polyps. J Allergy Clin Immunol. 2018;142(5):1489-99 e23.
27. Liao B, Cao PP, Zeng M, Zhen Z, Wang H, Zhang YN, et al. Interaction of thymic stromal lymphopoietin, IL-33, and their receptors in epithelial cells in eosinophilic chronic rhinosinusitis with nasal polyps. Allergy. 2015;70(9):1169-80.
28. Wang H, Hu DQ, Xiao Q, Liu YB, Song J, Liang Y, et al. Defective STING expression potentiates IL-13 signaling in epithelial cells in eosinophilic chronic rhinosinusitis with nasal polyps. J Allergy Clin Immunol. 2021;147(5):1692-703.
29. Zhang YN, Song J, Wang H, Wang H, Zeng M, Zhai GT, et al. Nasal IL-4(+)CXCR5(+) CD4(+) T follicular helper cell counts correlate with local IgE production in eosinophilic nasal polyps. J Allergy Clin Immunol. 2016;137(2):462-73.
30. de Borja Callejas F, Martinez-Anton A, Alobid I, Fuentes M, Cortijo J, Picado C, et al. Reconstituted human upper airway epithelium as 3-d in vitro model for nasal polyposis. PLoS One. 2014;9(6):e100537.
31. Soyka MB, Wawrzyniak P, Eiwegger T, Holzmann D, Treis A, Wanke K, et al. Defective epithelial barrier in chronic rhinosinusitis: the regulation of tight junctions by IFN-gamma and IL-4. J Allergy Clin Immunol. 2012;130(5):1087-96 e10.
32. Hu PS, Li T, Lin JF, Qiu MZ, Wang DS, Liu ZX, et al. VDR-SOX2 signaling promotes colorectal cancer stemness and malignancy in an acidic microenvironment. Signal Transduct Target Ther. 2020;5(1):183.
33. Hall DB, Vakkasoglu AS, Hales LM, Soliman TM. D-VITylation: Harnessing the biology of vitamin D to improve the pharmacokinetic properties of peptides and small proteins. Int J Pharm. 2022;624:122031.
34. Mulligan JK, Pasquini WN, Carroll WW, Williamson T, Reaves N, Patel KJ, et al. Dietary vitamin D3 deficiency exacerbates sinonasal inflammation and alters local 25(OH)D3 metabolism. PLoS One. 2017;12(10):e0186374.
35. Feldman D, Krishnan AV, Swami S, Giovannucci E, Feldman BJ. The role of vitamin D in reducing cancer risk and progression. Nat Rev Cancer. 2014;14(5):342-57.
36. Mostafa Bel D, Taha MS, Abdel Hamid T, Omran A, Lotfi N. Evaluation of vitamin D levels in allergic fungal sinusitis, chronic rhinosinusitis, and chronic rhinosinusitis with polyposis. Int Forum Allergy Rhinol. 2016;6(2):185-90.
37. Tomaszewska M, Sarnowska E, Rusetska N, Kowalik K, Sierdzinski J, Siedlecki JA, et al. Role of Vitamin D and Its Receptors in the Pathophysiology of Chronic Rhinosinusitis. J Am Coll Nutr. 2019;38(2):108-18.
38. Bikle D, Christakos S. New aspects of vitamin D metabolism and action - addressing the skin as source and target. Nat Rev Endocrinol. 2020;16(4):234-52.
39. Chauss D, Freiwald T, McGregor R, Yan B, Wang L, Nova-Lamperti E, et al. Autocrine vitamin D signaling switches off pro-inflammatory programs of T(H)1 cells. Nat Immunol. 2022;23(1):62-74.
40. Schedel M, Jia Y, Michel S, Takeda K, Domenico J, Joetham A, et al. 1,25D3 prevents CD8(+)Tc2 skewing and asthma development through VDR binding changes to the Cyp11a1 promoter. Nat Commun. 2016;7:10213.
41. Oh J, Matkovich SJ, Riek AE, Bindom SM, Shao JS, Head RD, et al. Macrophage secretion of miR-106b-5p causes renin-dependent hypertension. Nat Commun. 2020;11(1):4798.
42. Chen S, Sims GP, Chen XX, Gu YY, Chen S, Lipsky PE. Modulatory effects of 1,25-dihydroxyvitamin D3 on human B cell differentiation. J Immunol. 2007;179(3):1634-47.
43. Zhou Y, Dong B, Kim KH, Choi S, Sun Z, Wu N, et al. Vitamin D Receptor Activation in Liver Macrophages Protects Against Hepatic Endoplasmic Reticulum Stress in Mice. Hepatology. 2020;71(4):1453-66.
44. Bikle DD. Vitamin D metabolism, mechanism of action, and clinical applications. Chem Biol. 2014;21(3):319-29.
45. German B, Wei R, Hener P, Martins C, Ye T, Gottwick C, et al. Disrupting the IL-36 and IL-23/IL-17 loop underlies the efficacy of calcipotriol and corticosteroid therapy for psoriasis. JCI Insight. 2019;4(2).
46. Charoenngam N, Holick MF. Immunologic Effects of Vitamin D on Human Health and Disease. Nutrients. 2020;12(7).
47. Chen CL, Wang YT, Yao Y, Pan L, Guo B, Zhu KZ, et al. Inflammatory Endotypes and Tissue Remodeling Features in Antrochoanal Polyps. Allergy, asthma & immunology research. 2021;13(6):863-81.
48. Bosse Y, Lemire M, Poon AH, Daley D, He JQ, Sandford A, et al. Asthma and genes encoding components of the vitamin D pathway. Respir Res. 2009;10(1):98.
49. Raby BA, Lazarus R, Silverman EK, Lake S, Lange C, Wjst M, et al. Association of vitamin D receptor gene polymorphisms with childhood and adult asthma. Am J Respir Crit Care Med. 2004;170(10):1057-65.
50. Shan L, Kang X, Liu F, Cai X, Han X, Shang Y. Expression of vitamin D receptor in bronchial asthma and its bioinformatics prediction. Mol Med Rep. 2018;18(2):2052-60.
51. Kilic M, Ecin S, Taskin E, Sen A, Kara M. The

Vitamin D Receptor Gene Polymorphisms in Asthmatic Children: A Case-Control Study. Pediatr Allergy Immunol Pulmonol. 2019;32(2):63-9.
52. Mues N, Martin RJ, Alam R, Schaunaman N, Dimasuay KG, Kolakowski C, et al. Bacterial DNA amplifies neutrophilic inflammation in IL-17-exposed airways. ERJ Open Res. 2023;9(1).
53. Rafique A, Rejnmark L, Heickendorff L, Moller HJ. 25(OH)D3 and 1.25(OH)2D3 inhibits TNF-alpha expression in human monocyte derived macrophages. PLoS One. 2019;14(4):e0215383.
54. Hashemian F, Sadegh S, Jahanshahi J, Seif Rabiei MA, Hashemian F. Effects of Vitamin D Supplementation on Recurrence of Nasal Polyposis after Endoscopic Sinus Surgery. Iran J Otorhinolaryngol. 2020;32(108):21-8.
55. Ghazavi H, Hashemi SM, Jafari S. The Effect of Vitamin D Supplement on the Relapsing Incidence of Rhinosinusitis with Nasal Polyposis after Fuctional Endoscpoic Sinus Surgery. Adv Biomed Res. 2023;12:29.
56. Baruah B, Gupta A, Kumar A, Kumar A. The role of oral vitamin D3 supplementation in the treatment of Chronic Rhinosinusitis in adults with Vitamin D deficiency. J Family Med Prim Care. 2020;9(6):2877-9.

Zheng Liu, M.D., Ph.D.
Department of Otolaryngology
Head and Neck Surgery
Tongji Hospital
Tongji Medical College
Huazhong University of Science and Technology
No. 1095 Jiefang Avenue
Wuhan 430030
China

Tel: +86-27-8366 2606
Fax: +86-27-8366 2606
E-mail: zhengliuent@hotmail.com

This manuscript contains online supplementary material

SUPPLEMENTARY MATERIAL

METHODS

Subjects

This study was approved by the Ethics Committee of Tongji Hospital of Huazhong University of Science and Technology, and written informed consent was obtained from every participant. A total of 212 patients including 75 control subjects, 70 patients with eosinophilic chronic rhinosinusitis with nasal polyps (CRSwNP), and 67 patients with noneosinophilic CRSwNP were enrolled in this study. CRSwNP was diagnosed based on the current American and European guidelines[1, 2]. Eosinophilic and noneosinophilic CRSwNP were defined according to whether the percent of tissue eosinophils exceeded 10% of total infiltrating cells, as reported by our previous study[3]. This cutoff was calculated as twice the standard deviation of the mean eosinophil percentage in control subjects[3]. Control subjects were those undergoing septoplasty due to anatomic variations and without other sinonasal diseases. All subjects came from central China and CRSwNP patients had bilateral nasal polyps.

Patients' atopic status was evaluated by skin prick tests with a standard panel of common inhalant allergens, and/or by using the ImmunoCAP (Phadia, Uppsala, Sweden) to detect IgE levels against common inhalant allergens in our region[4, 5]. The diagnosis of allergic rhinitis was made based on the concordance between the atopic status and typical allergic symptoms. Asthma was diagnosed based on history and physician's diagnosis according to Global Initiative for Asthma 2006 guideline[6]. Oral glucocorticoids and intranasal steroid sprays were discontinued at least 3 months and 1 month before surgery, respectively. Antileukotrienes were discontinued at least 1 month before inclusion. None received VD3 supplement within 3 months before surgery. Patients with an acute upper respiratory tract infection and acute asthma episode within 4 weeks before enrollment, as well as those who were receiving immunotherapy or biologics treatment were excluded. In addition, patients with a history of aspirin sensitivity, antrochoanal polyps, fungal sinusitis, cystic fibrosis, primary ciliary dyskinesia, immunodeficiency, or systemic vasculitis were excluded from this study, because these are discrete disorders with unique pathophysiology. The details of subjects' characteristics are outlined in Table S1.

Nasal polyp (NP) tissues from CRSwNP patients and inferior turbinate mucosal tissues from control subjects were collected during surgery, respectively. Human nasal epithelial cells (HNECs) were scraped from NPs of CRSwNP patients and from middle meatus of control subjects using a sterile Rhino-Pro curette (Arlington Scientific Inc, Springville, UT)[7, 8]. Each nasal scraping specimen yielded 1-2×10^6 cells, of which more than 95% were epithelial cells[9]. Not all samples were included in every experiment protocol due to the limited quantity of samples available. The exact number of samples used in each experiment were provided in figures or figure legends.

Histology and immunofluorescence

Tissue samples were fixed in 4% formaldehyde solution and embedded in paraffin. Paraffin sections (4 μm) were prepared from paraffin-embedded human nasal tissue blocks. After deparaffinization and rehydration, sections were stained with hematoxylin and eosin routinely for histology examination and to count the number of eosinophils and total inflammatory cells at high-power magnification as previously reported[3].

The expression of vitamin D receptor (VDR) and 1a-hydroxylase (cytochrome P450 family 27 subfamily B member 1, CYP27B1) in NPs as well as their co-localization on hematopoietic cells were assessed by immunofluorescence staining as previously reported[7, 8, 10]. Briefly, sections were subjected to heat-induced epitope retrieval using Target Retrieval Solution (Dako, Carpinteria, Calif, USA) and 5% bovine serum albumin (Guge Biotechnology, Wuhan, China) was used to block nonspecific binding[7, 8, 10]. Specific primary antibodies (Table S2) were subsequently applied to the sections with an overnight incubation at 4°C, followed by incubation with fluorescence-conjugated secondary antibodies (Table S3) for 1 hour at room temperature. After that, sections were stained with DAPI at room temperature for 5 minutes[8, 10]. Species- and subtype-matched antibodies were used as negative controls. The relationships between VDR and CYP27B1 positive cells and myeloperoxidase (MPO), eosinophil peroxidase (EPX), CD3, CD11c, CD20, CD68, CD138, and tryptase positive cells were assessed by double immunofluorescence staining. The intensity of positive staining in epithelial cells was analyzed by using image pro-plus 6.0 analysis software (Media Cybernetics, Inc. Silver Spring, MD, USA) and the results were expressed as average optical density value per unit area[11, 12].

The numbers of MPO^+ neutrophils and major basic protein $(MBP)^+$ eosinophils were counted at high-power magnification (400×). Ten high-power fields (HPFs) were randomly chosen and counted by two independent observers, in a blinded fashion[13].

ELISA

Tissue samples were weighted and 1 mL of 0.9% sodium chloride solution supplemented with 10 μL of 100 mM phenylmethylsulfonyl fluoride was added per 0.1 g tissue[14]. Tissue was homogenized on ice and centrifuged at 3,000 rpm for 10 minutes at 4°C. Freshly obtained peripheral blood were centrifuged at 3,000 rpm for 10 minutes. Tissue lysates, serum, cell and ex vivo nasal explant culture supernatants were harvested and stored at -80°C for further analysis. The levels of 25-hydroxyvitamin D3 (25VD3), 1,25-hydroxyvitamin D3 (1,25VD3), IL-36γ, IL-5,

IL-17A, and interferon γ (IFN-γ) in nasal tissue lysates, serum or culture supernatants were measured using commercially accessible ELISA kits according to manufactures' instruction, and the lower detection limit was presented in Table S4. The total tissue protein levels were quantified via a BCA detection kit (Guge Biotechnology), and the levels of 25VD3 and cytokine in nasal tissue lysates were expressed as a protein concentration per mg of total protein.

Quantitative RT-PCR

Total RNA was extracted from tissues and cells by employing TRIzol reagent (TaKaRa Biotechnology, Dalian, China) as mentioned previously[3, 14, 15]. 1 μg of total RNA was reverse-transcribed to cDNA using a PrimeScript RT reagent kit (TaKaRa Biotechnology). cDNA equivalent to 50 ng of total RNA was used for PCR assay. Quantitative PCR was performed by using the SYBR Premix Ex Taq kit (TaKaRa Biotechnology) with specific primers (Table S5) on StepOnePlus device (Applied Biosystems, Foster City, Calif). Amplification was as follows: 95°C for 2 minutes, followed by 40 cycles of 95°C for 10 seconds, specific annealing temperature for 10 seconds, and 72°C for 15 seconds. After PCR, a melting curve was constructed by increasing the temperature from 65 to 95°C with a temperature transition rate of 0.1°C/s. Relative gene expression was calculated by using the 2(-ΔΔ CT) method[16]. A normal inferior turbinate mucosal sample and a control cell culture sample were utilized as the calibrator for tissue samples and cell culture samples, respectively. Beta-glucuronidase (GUSB) was used as a housekeeping gene for normalization of gene expression. No template sample was used as negative control.

Western blotting

Total cellular protein was extracted from tissues and HNECs in modified Radio-Immunoprecipitation Assay (RIPA) Buffer (Guge Biotechnology) containing 2% cocktail of protease inhibitors (Guge Biotechnology) as previously stated[7]. Protein concentrations were quantified by using a bicinchoninic acid protein assay kit (Guge Biotechnology). Samples containing 30 μg of proteins were denatured by 10% sodium dodecyl sulfate-polyacrylamide gel electrophoresis (SDS-PAGE) and then transferred to polyvinyl difluoride membranes (Guge Biotechnology). To block non-specific binding, the membranes were incubated with 5% fat-free skim milk in Tris-buffered saline with Tween-20 (TBS-T; Guge Biotechnology) for 1 hour at room temperature and then incubated overnight at 4°C with primary antibodies as listed in Table S6. After washing 3 times in TBS-T buffer, the membranes were incubated with horseradish peroxidase-conjugated secondary antibody (goat anti-rabbit IgG, 1:3000, Guge Biotechnology) and finally processed by using an ECL chemiluminescence reaction kit (Cell Signaling, Danvers, MA, USA), followed by exposure on chemiluminescent film to visualize the proteins. β-actin quantification was used as an internal standard to adjust for discrepancies in total protein loading. Densitometric analysis of the blots was undertaken by utilizing the software AlphaEase FC (Alpha Innotech, Silicon Valley, CA, USA). CYP27B1 and VDR were identified as a single band around 57 KDa and 48 KDa, respectively.

Dispersed nasal tissue cell preparation and flow cytometry

Dispersed nasal tissue cells were prepared from freshly obtained sinonasal tissues by means of mechanical dissociation with GentleMACS Dissociator (Miltenyi Biotec, San Diego, CA, USA)[7, 8]. The resulting single cell suspension was filtered 2 times through a 40 μm cell strainer (BD Biosciences, San Jose, CA, USA) and washed twice with RPMI-1640 medium (HyClone Laboratories, Chicago, IL, USA)[7]. Cell pellets were suspended in erythrocyte lysis buffer and incubated for 5 minutes to remove red blood cells. After washing with phosphate-buffered saline (PBS), cells were resuspended in RPMI-1640 medium. For flow cytometry analysis, cells were stained with fixable viability stain 700 (BD Biosciences) to exclude dead cells. Cells were then incubated for surface staining with APC-conjugated mouse monoclonal antibody against human CD326 and BV421-conjugated mouse monoclonal antibody against human CD45 for 30 minutes at 4°C in the dark. For intracellular staining of VDR and CYP27B1, cells were fixed and permeabilized using the BD cytofix/cytoperm kit (BD Biosciences) according to manufacturer's protocols after CD45 and CD326 staining. Cells were then stained with rabbit polyclonal antibody against human VDR (1 μg/mL, Abcam, Cambridge, UK) and CYP27B1 (1 μg/mL, Abcam), respectively. After incubating for 30 minutes in the dark at 4°C, cells were incubated with FITC-conjugated F(ab')2 donkey anti-rabbit IgG H&L antibody (1:200, Biolegend, San Diego, CA, USA) for another 30 minutes. The detailed information of antibodies used for flow cytometry is listed in Table S7. Species and subtype-matched antibodies were used as negative controls. After staining, cells were analyzed by using BD FACSCelesta flow cytometer (Becton Dickinson Biosciences, San Jose, CA, USA). The data were analyzed using FlowJo software (TreeStar, Ashland, OR, USA).

Cell culture and treatment

HNECs were scraped from middle meatus of control subjects and polyp of NPs and were cultured with an air-liquid interface (ALI) method or submerged as mentioned elsewhere[15, 17-19]. For ALI culture, the obtained HNECs were washed twice in Dulbecco modified Eagle medium (Thermo Fisher Scientific, Waltham, MA, USA) with penicillin/streptomycin (Invitrogen, Carlsbad, CA, USA) and then grown submerged in bronchial epithelial cell basal medium (BEBM, Lonza, Walkersville, MD, USA) supplemented with SingleQuot Kit Suppl (Lonza) in 6-well plates pre-coated with rat tail collagen type I (Sigma-Aldrich, St. Louis, MO, USA) in a 5% CO_2-humidified atmosphere at 37°C. Upon confluence, the cells were seeded onto gel-coated 0.4 μm transwell culture inserts (Millipore Corp, Billerica, MA, USA) and were grown in

bronchial epithelial cell growth medium (Lonza). When they were confluent, medium from the apical side of the culture was removed and medium below the insert was replenished with an ALI culture medium consisting of BEBM and Dulbecco's modified Eagle's medium H (50: 50; Invitrogen). HNECs were cultured at ALI method for 21 days for the differentiation[18]. After the HNECs were differentiated, they were stimulated with IL-4, IL-6, IL-10, IL-12, IL-13, IL-17A, TNF-α, IL-1β, IFN-γ, and IL-22 at 10 ng/mL (R&D systems, Minneapolis, MN, USA), poly (I:C) (dsRNA) at 25 μg/mL (Tocris, Bristol, UK), lipopolysaccharides (LPS) (InvivoGen, San Diego, CA, USA) at 1 μg/mL, staphylococcal enterotoxin B (SEB) (Millipore, Merck KGaA, Darmstadt, Germany) at 1 μg/mL, CpG (InvivoGen) at 2 μg/mL, *Dermatophagoides pteronyssinus* group 1 (Der p1) at 10 μg/mL (Prospec, East Brunswick, NJ, USA), 1,25VD3 at 100 nM (MedChemExpress, NJ, USA), or 25VD3 at 100 nM (MedChemExpress) in BEBM free of steroids for 6, 24 or 48 hours[20]. After treatment, HNECs were harvested for quantitative RT-PCR assay or RNA sequencing analysis. Culture supernatants and cell lysates were collected for ELISA and western blotting, respectively.

In some experiments, when assessing the differences among the control, eosinophilic CRSwNP, and noneosinophilic CRSwNP groups, HNECs scraped from different study groups were cultured submerged to maintain the disease-specific expression pattern of CYP27B1. For submerged culture, HNECs were cultured in BEBM (Lonza) in 6-well plates pre-coated with rat tail collagen type I (Sigma-Aldrich) in a 5% CO_2-humidified atmosphere at 37°C as previously described[7]. When submerge cultured HNECs reached 80% confluence, cells were treated with 25VD3 (100 nM, MedChemExpress). After 24-hour treatment, culture supernatants were collected for ELISA. For luciferase report experiments, HNECs from control subjects were submerged cultured.

For the siRNA transfection experiments, HNECs were cultured with an ALI method. At the 14th, 17th and 21th day of differentiation, the HNECs maintained in ALI culture were pretreated with epidermal growth factor (100 μg/mL, Sigma-Aldrich), a known enhancer of macropinocytosis, for 15 minutes and then were transfected with CYP27B1 siRNA (siCYP27B1, 100 nM; RiBo Biotechnology, Guangzhou, China) or the corresponding negative control siRNA (siNC, 100 nM) by using Lipofectamine 3000 transfection agent (Thermo Fisher Scientific) under the manufacturer's instruction for 24 hours. After 24-hour recovery period, the medium was refreshed, and the cells were treated with 25VD3 (100 nM, MedChemExpress). After 24-hour or 48-hour treatment, HNECs were harvested for quantitative RT-PCR assay and culture supernatants were collected for ELISA. The sense sequence are as follows: CYP27B1 siRNA, 5'-ACCCTGAACAACGTAGTCT-3', and scrambled siRNA was used as negative control (siNC).

Promoter-luciferase reporter construct and luciferase assay

Putative VDR-binding elements on the *IL36G* promoter were analytically anticipated employing the JASPAR database (http://jaspar.binf.ku.dk/). DNA fragments containing wild-type and mutated VDR binding sites of *IL36G* promoter were generated by PCR and were cloned into firefly luciferase reporter constructs (pGL3 vector; Promega, Madison, WI, USA). The four mutated constructs included *IL36G* pGL3-MUT1 (-1683 to -1676 site), *IL36G* pGL3-MUT2 (-873 to -866 site), *IL36G* pGL3-MUT3 (-814 to -807 site), and *IL36G* pGL3-MUT4 (-292 to -285 site). For luciferase report experiments, HNECs from control subjects were submerged cultured and transfected with the VDR overexpression plasmid, pcVDR (GenBank accession no.NM_000376.3; 2 μg, Qijing Biological Technology, Wuhan, China), and its control plasmid pcDNA3.1 (Qijing Biological Technology) using Lipofectamine 3000 transfection agent (Thermo Fisher Scientific) under the manufacturer's instruction for 24 hours and subsequently transfected with the wild-type or mutated constructs (1 μg per well, Qijing Biological Technology) together with the renilla luciferase plasmid (200 ng per well, Qijing Biological Technology). Twenty-four hours later, cell lysates were harvested by passive lysis buffer (Promega) and the luciferase activity was measured and analyzed using a dual luciferase reporter assay kit (Promega).

Ex vivo polyp explant culture

NP tissues from 5 patients with eosinophilic CRSwNP and 5 patients with noneosinophilic CRSwNP were obtained during surgery and cut into multiple samples of approximately 6 mm^3 for tissue culture as described previously[21, 22]. Briefly, sections of tissue were placed on 0.4 μm well inserts (Millipore Corp) in 2 mL of Dulbecco modified Eagle medium/F-12 (Thermo Fisher Scientific) supplemented with 2 mM L-glutamine, 100 U/mL penicillin, and 100 μg/mL streptomycin (Invitrogen)[23]. The tissues were oriented with the epithelium being exposed to the air, forming an air–liquid interface to mimic the in vivo situation. Tissues were incubated in the absence or presence of 1,25VD3 (100 nM, MedChemExpress), 25VD3 (100 nM, MedChemExpress), and dexamethasone (10^{-6} M, USBiological, Swampscott, MA, USA). NP explants were cultured at 37°C with 5% CO_2 in humidified air for 24 or 48 hours. After stimulation, tissue explants and cell culture supernatants were harvested and subjected to quantitative RT-PCR and ELISA, respectively.

RNA sequencing

HNECs obtained from 3 control patients were cultured with ALI and treated with or without 1,25VD3 (100 nM, MedChemExpress) for 6 hours. After culture, total RNA was extracted from cells using TRIzol (TaKaRa Biotechnology), with 5 μg of RNA per sample used as input material for the RNA sample preparation. RNA integrity and concentration were assessed with an Agilent 2100 Bioanalyzer and an RNA Nano 6000 Assay Kit (Agilent Technologies, Santa Clara, CA, USA). Sequencing libraries were gene-

rated according to the manufacturer's protocol with index codes appended to attribute sequences to each sample. Briefly, mRNA was purified from total RNA using poly-T oligo-attached magnetic beads. Fragmentation was carried out using divalent cations under elevated temperature by using NEBNext RNA Library Prep Kit (NEB). First strand cDNA was synthesized using random hexamer primer and RNase H, followed by the synthesis of the second strand cDNA. The library fragments were purified with QiaQuick PCR kits (QIAGEN, Duesseldorf, Germany) and eluted with EB buffer. Subsequently, the terminal repair, A-tailing, and adapter adding were implemented and the desired products were retrieved, which were subjected to PCR amplification. The library quality was evaluated by an Agilent 2100 Bioanalyzer system (Agilent Technologies) and the final library products were deeply sequenced on an Illumina NovaSeq6000 S4 platform with 150 bp paired-end reads by Annoroad Gene Technology (Beijing). In order to analyze differential gene expression, the fragments count of unambiguous clean tags for each gene was calculated by using FPKM (Fragments per Kilobase of transcript per Millon Mapped Fragments) method[24]. The DESeq R package (v1.18.0) software was used to analyze the differential gene expression between two groups. Genes with P-value < 0.05 and fold-change ≥ 1.5 between two groups were considered significantly different. The RNA-Seq primary data have been submitted to the NCBI repository SRA (Bioproject accession: PRJNA889463).

References

1. Fokkens WJ, Lund VJ, Hopkins C, Hellings PW, Kern R, Reitsma S, et al. European Position Paper on Rhinosinusitis and Nasal Polyps 2020. Rhinology. 2020;58(Suppl S29):1-464.
2. Orlandi RR, Kingdom TT, Smith TL, Bleier B, DeConde A, Luong AU, et al. International consensus statement on allergy and rhinology: rhinosinusitis 2021. Int Forum Allergy Rhinol. 2021;11(3):213-739.
3. Cao PP, Li HB, Wang BF, Wang SB, You XJ, Cui YH, et al. Distinct immunopathologic characteristics of various types of chronic rhinosinusitis in adult Chinese. J Allergy Clin Immunol. 2009;124(3):478-84, 84 e1-2.
4. Wang Y, Chen H, Zhu R, Liu G, Huang N, Li W, et al. Allergic Rhinitis Control Test questionnaire-driven stepwise strategy to improve allergic rhinitis control: a prospective study. Allergy. 2016;71(11):1612-9.
5. Qi S, Chen H, Huang N, Li W, Liu G, Wang Y, et al. Early intervention improves clinical responses to house dust mite immunotherapy in allergic rhinitis patients. Int Arch Allergy Immunol. 2016;171(3-4):234-40.
6. Bateman ED, Hurd SS, Barnes PJ, Bousquet J, Drazen JM, FitzGerald JM, et al. Global strategy for asthma management and prevention: GINA executive summary. Eur Respirat J. 2008;31(1):143-78.
7. Wang H, Hu DQ, Xiao Q, Liu YB, Song J, Liang Y, et al. Defective STING expression potentiates IL-13 signaling in epithelial cells in eosinophilic chronic rhinosinusitis with nasal polyps. J Allergy Clin Immunol. 2021;147(5):1692-703.
8. Wang H, Li ZY, Jiang WX, Liao B, Zhai GT, Wang N, et al. The activation and function of IL-36gamma in neutrophilic inflammation in chronic rhinosinusitis. J Allergy Clin Immunol. 2018;141(5):1646-58.
9. Lee HS, Myers A, Kim J. Vascular endothelial growth factor drives autocrine epithelial cell proliferation and survival in chronic rhinosinusitis with nasal polyposis. Am J Respir Crit Care Med. 2009;180(11):1056-67.
10. Song J, Wang H, Zhang YN, Cao PP, Liao B, Wang ZZ, et al. Ectopic lymphoid tissues support local immunoglobulin production in patients with chronic rhinosinusitis with nasal polyps. J Allergy Clin Immunol. 2018;141(3):927-37.
11. Gu J, Liang Y, Qiao L, Li X, Li X, Lu Y, et al. Expression analysis of URI/RMP gene in endometrioid adenocarcinoma by tissue microarray immunohistochemistry. Int J Clin Exp Pathol. 2013;6(11):2396-403.
12. Liu JX, Chen AN, Yu Q, Shi KT, Liu YB, Guo CL, et al. MEX3B inhibits collagen production in eosinophilic nasal polyps by downregulating epithelial cell TGFBR3 mRNA stability. JCI Insight. 2023;8(9).
13. Chen CL, Wang YT, Yao Y, Pan L, Guo B, Zhu KZ, et al. Inflammatory endotypes and tissue remodeling features in antrochoanal polyps. Allergy Asthma Immunol Res. 2021;13(6):863-81.
14. Cao PP, Zhang YN, Liao B, Ma J, Wang BF, Wang H, et al. Increased local IgE production induced by common aeroallergens and phenotypic alteration of mast cells in Chinese eosinophilic, but not non-eosinophilic, chronic rhinosinusitis with nasal polyps. Clin Exp Allergy. 2014;44(5):690-700.
15. Zhang XH, Zhang YN, Li HB, Hu CY, Wang N, Cao PP, et al. Overexpression of miR-125b, a novel regulator of innate immunity, in eosinophilic chronic rhinosinusitis with nasal polyps. Am J Respir Crit Care Med. 2012;185(2):140-51.
16. Livak KJ, Schmittgen TD. Analysis of relative gene expression data using real-time quantitative PCR and the 2(-Delta Delta C(T)) Method. Methods. 2001;25(4):402-8.
17. Liao B, Cao PP, Zeng M, Zhen Z, Wang H, Zhang YN, et al. Interaction of thymic stromal lymphopoietin, IL-33, and their receptors in epithelial cells in eosinophilic chronic rhinosinusitis with nasal polyps. Allergy. 2015;70(9):1169-80.
18. Soyka MB, Wawrzyniak P, Eiwegger T, Holzmann D, Treis A, Wanke K, et al. Defective epithelial barrier in chronic rhinosinusitis: the regulation of tight junctions by IFN-gamma and IL-4. J Allergy Clin Immunol. 2012;130(5):1087-96 e10.
19. de Borja Callejas F, Martinez-Anton A, Alobid I, Fuentes M, Cortijo J, Picado C, et al. Reconstituted human upper airway epithelium as 3-d in vitro model for nasal polyposis. PLoS One. 2014;9(6):e100537.
20. Liu Z, Lu X, Zhang XH, Bochner BS, Long XB, Zhang F, et al. Clara cell 10-kDa protein expression in chronic rhinosinusitis and its cytokine-driven regulation in sinonasal mucosa. Allergy. 2009;64(1):149-57.
21. Liu Z, Lu X, Wang H, You XJ, Gao QX, Cui YH. Group II subfamily secretory phospholipase A2 enzymes: expression in chronic rhinosinusitis with and without nasal polyps. Allergy. 2007;62(9):999-1006.
22. Hauber HP, Daigneault P, Frenkiel S, Lavigne F, Hung HL, Levitt RC, et al. Niflumic acid and MSI-2216 reduce TNF-alpha-induced mucin expression in human airway mucosa. J Allergy Clin Immunol. 2005;115(2):266-71.
23. Sha Q, Truong-Tran AQ, Plitt JR, Beck LA, Schleimer RP. Activation of airway epithelial cells by toll-like receptor agonists. Am J Respir Cell Mol Biol. 2004;31(3):358-64.
24. Mortazavi A, Williams BA, McCue K, Schaeffer L, Wold B. Mapping and quantifying mammalian transcriptomes by RNA-Seq. Nat Methods. 2008;5(7):621-8.

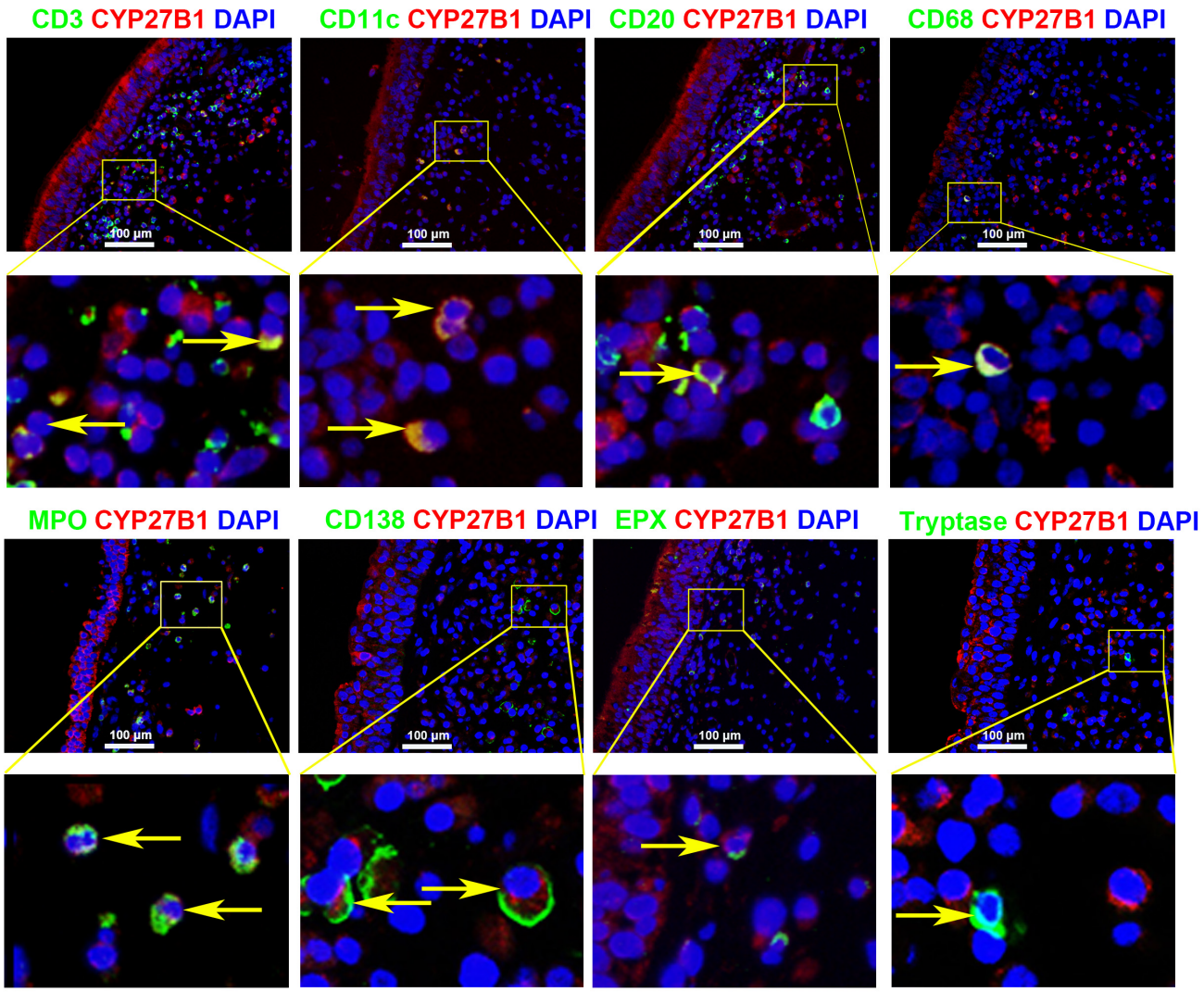

Figure S1. CYP27B1 expression in infiltrating immune cells in nasal polyps. Double immunofluorescence staining of nasal polyp tissue sections demonstrates that CYP27B1 is expressed by $CD3^+$ T cells, $CD11c^+$ dendritic cells, $CD20^+$ B cells, $CD68^+$ macrophages, MPO^+ neutrophils, $CD138^+$ plasma cells, and weakly expressed by EPX^+ eosinophils, but not by $tryptase^+$ mast cells in nasal polyps. Representative photomicrographs are shown (original magnification × 400). Scale bar, 100 μm. The below images show higher magnification of the outlined area. Arrows indicate the representative positive cells. CYP27B1, cytochrome P450 family 27 subfamily B member 1; EPX, eosinophil peroxidase; MPO, myeloperoxidase; DAPI, 4'6-diamidino-2-phenylindole dihydrochloride.

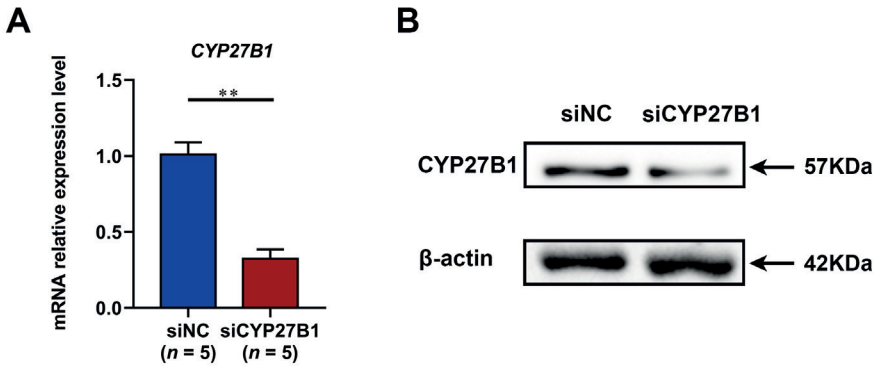

Figure S2. The transfection efficiency of siCYP27B1 in HNECs. HNECs from control subjects were cultured with an air-liquid interface method and transfected with siCYP27B1 or control siRNA (siNC) (n = 5). The transfection efficiency of siCYP27B1 was confirmed at mRNA (A) and protein (B) expression levels by RT-PCR and western blotting, respectively. Representative blots are shown. **P < 0.01. CYP27B1, cytochrome P450 family 27 subfamily B member 1.

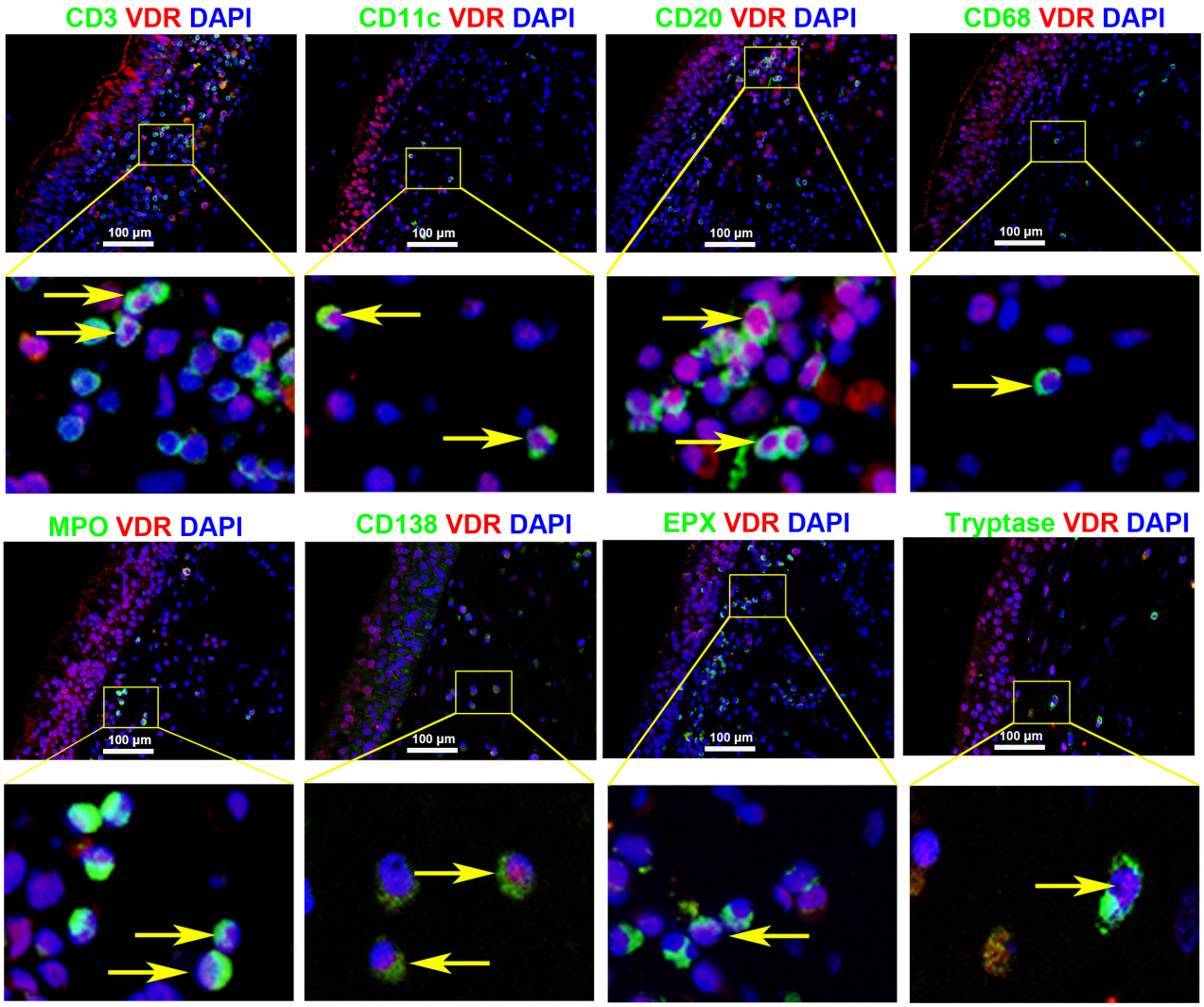

Figure S3. VDR expression in infiltrating immune cells in nasal polyps. Double immunofluorescence staining of nasal polyp tissue sections demonstrates that VDR is expressed by $CD3^+$ T cells, $CD11c^+$ dendritic cells, $CD20^+$ B cells, $CD68^+$ macrophages, MPO^+ neutrophils, $CD138^+$ plasma cells, and weakly expressed by EPX^+ eosinophils and $tryptase^+$ mast cells in nasal polyps. Representative photomicrographs are shown (original magnification × 400). Scale bar, 100 μm. The below images show higher magnification of the outlined area. Arrows indicate the representative positive cells. VDR, vitamin D receptor; EPX, eosinophil peroxidase; MPO, myeloperoxidase; DAPI, 4'6-diamidino-2-phenylindole dihydrochloride.

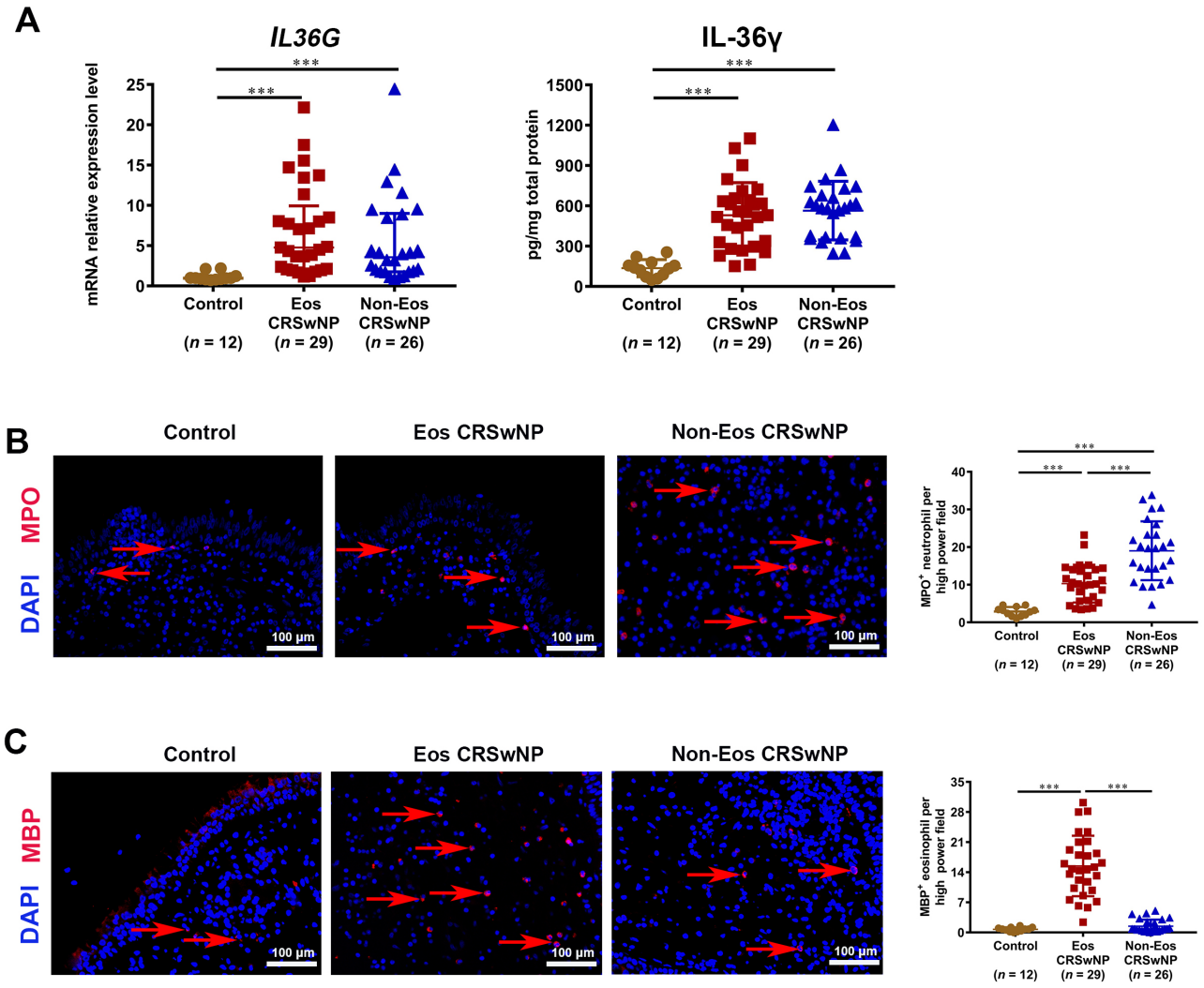

Figure S4. IL-36γ expression and eosinophil and neutrophil infiltration in nasal polyps. (A) The mRNA and protein levels of IL-36γ in nasal tissues in different study groups as detected by quantitative RT-PCR and ELISA, respectively. (B and C) Immunofluorescence staining (left) and quantification (right) of MPO$^+$ neutrophils (B) and MBP$^+$ eosinophils (C) in sinonasal mucosa (original magnification × 400). Scale bar, 100 μm. ***P < 0.001. CRSwNP, chronic rhinosinusitis with nasal polyps; Eos, eosinophilic; Non-Eos, noneosinophilic; MPO, myeloperoxidase; MBP, major basic protein; DAPI, 4'6-diamidino-2-phenylindole dihydrochloride.

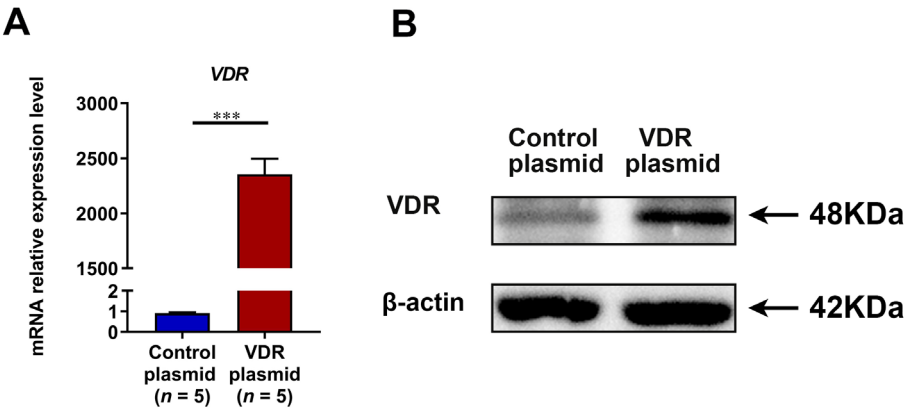

Figure S5. The transfection efficiency of VDR overexpression plasmid in HNECs. HNECs from control subjects were cultured submerged and transfected with the VDR overexpression plasmid pcVDR or control plasmid pcDNA3.1 (n = 5). The transfection efficiency of VDR overexpression plasmid was confirmed at mRNA (A) and protein (B) expression levels by RT-PCR and western blotting, respectively. Representative blots are shown. ***P < 0.001. VDR, vitamin D receptor.

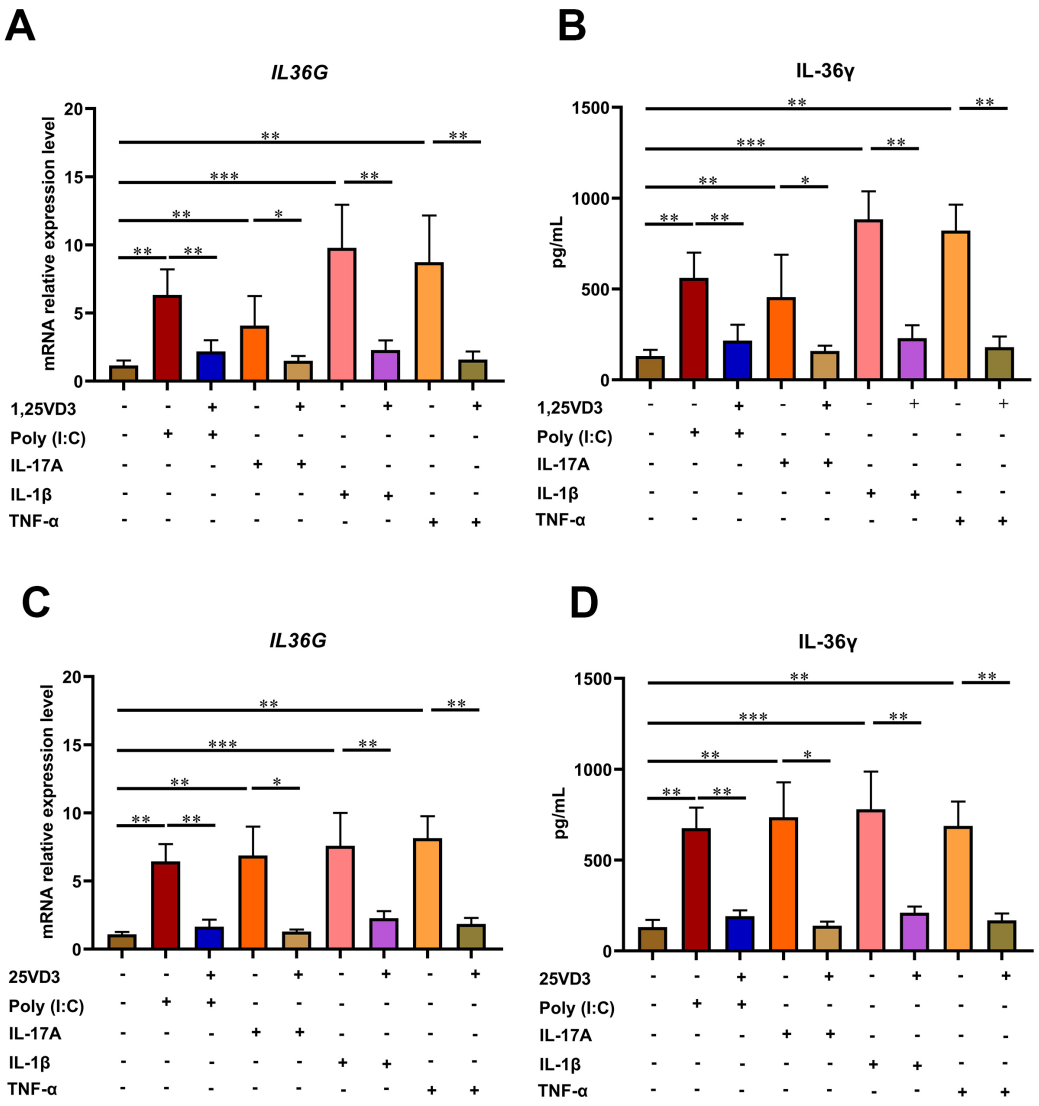

Figure S6. IL-36γ induction by inflammatory stimulus is suppressed by 1,25VD3 and 25VD3 in nasal epithelial cells. HNECs obtained from control subjects were cultured with an air-liquid interface method (n = 5). (A and B) HNECs were stimulated with 1,25VD3 in the presence of poly (I:C), IL-17A, IL-1β, or TNF-α. IL-36γ mRNA expression levels in HNECs and protein levels in culture supernatants were detected by RT-PCR (A) or ELISA (B), respectively. C and D, HNECs were stimulated with 25VD3 in the presence of poly (I:C), IL-17A, IL-1β, or TNF-α. IL-36γ mRNA expression levels in HNECs and protein levels in culture supernatants were detected by RT-PCR (C) and ELISA (D), respectively. *P < 0.05, **P < 0.01, and ***P < 0.001.

Table S1. The demographic characteristics of subjects.

	Control	Eos CRSwNP	Non-Eos CRSwNP	P value
Total subjects enrolled	75	70	67	
Methodology used				
Immunofluorescence				
Subject number	18	35	32	
Gender, male	12 (67%)	18 (51%)	23 (72%)	0.206
Age (years)	33 (28, 42)	46 (30, 54)	42 (28, 53)	0.110
Patients with atopy	0 (0)	6 (17%)	4 (13%)	0.183
Patients with AR	1 (6%)	4 (11%)	1 (3%)	0.399
Patients with asthma	0 (0)	2 (6%)	0 (0)	0.510
RT-PCR and ELISA				
Subject number	12	29	26	
Gender, male	9 (75%)	17 (59%)	16 (62%)	0.607
Age (years)	33 (26, 45)	47 (30, 54)	46 (38, 54)	0.090
Patients with atopy	0 (0)	5 (17%)	2 (8%)	0.219
Patients with AR	0 (0)	3 (10%)	1 (4%)	0.515
Patients with asthma	0 (0)	2 (7%)	0 (0)	0.659
Flow cytometry				
Subject number	16	16	16	
Gender, male	12 (75%)	11 (69%)	11 (69%)	0.904
Age (years)	39 (32, 46)	40 (37, 48)	41 (34, 46)	0.668
Patients with atopy	1 (6%)	3 (19%)	1 (6%)	0.409
Patients with AR	0 (0)	2 (13%)	0 (0)	0.319
Patients with asthma	0 (0)	1 (6%)	0 (0)	1.000
Western blot				
Subject number	9	9	9	
Gender, male	7 (78%)	6 (67%)	5 (56%)	0.607
Age (years)	35 (27, 46)	46 (35,55)	43 (33, 55)	0.276
Patients with atopy	0 (0)	2 (22%)	1 (11%)	0.325
Patients with AR	0 (0)	1 (11%)	0 (0)	1.000
Patients with asthma	0 (0)	1 (11%)	0 (0)	1.000
Cell culture study				
Subject number	32	5	5	
Gender, male	23 (72%)	3 (60%)	3 (60%)	0.778
Age (years)	33 (27, 40)	42 (33, 50)	46 (28, 56)	0.140
Patients with atopy	2 (6%)	1 (20%)	1 (20%)	0.236
Patients with AR	0 (0)	1 (20%)	0 (0)	0.238
Patients with asthma	0 (0)	0 (0)	0 (0)	-
Polyp explant culture study				
Subject number	-	5	5	
Gender, male	-	2 (40%)	3 (60%)	0.527
Age (years)	-	40 (27, 52)	46 (24, 51)	0.952
Patients with atopy	-	1 (20%)	1 (20%)	1.000
Patients with AR	-	0 (0)	0 (0)	-
Patients with asthma	-	0 (0)	0 (0)	-

For continuous variables, results are expressed as medians and interquartile ranges. Categorical variables are summarized using percentage, and analyzed by Chi-square or Fisher's exact test. CRSwNP, chronic rhinosinusitis with nasal polyps; AR, allergic rhinitis.

Table S2. Primary antibodies used in immunofluorescence.

Antibody	Species	Concentration	Clone ID	Reference	Source
VDR	Rabbit	1:100	polyclonal	GTX104615	GeneTex, Irvine, CA, USA
CYP27B1	Rabbit	1:100	ERP20271	Ab206655	Abcam, Cambridge, UK
MPO	Mouse	1:100	2C7	Ab25989	Abcam
EPX	Mouse	1:100	EPO104	NBP2-32844-0	Novus Biologicals, CO, USA
MBP	Rabbit	1:100	polyclonal	Ab187523	Abcam
CD3	Mouse	1:100	B1.1	TA320268	Zhongshan Golden Bridge Biotechnology, Beijing, China
CD11c	Mouse	1:100	FK24	Ab23602	Abcam
CD68	Mouse	1:100	KP1	ZM-0060	Zhongshan Golden Bridge Biotechnology
CD20	Mouse	1:100	OTI1H4	TA800394	Zhongshan Golden Bridge Biotechnology
CD138	Mouse	1:100	B-A38	Ab34164	Abcam
Tryptase	Mouse	1:100	AA	Ab2378	Abcam

VDR, vitamin D receptor; CYP27B1, cytochrome P450 family 27 subfamily B member 1; MBP, major basic protein; MPO, myeloperoxidase; EPX, eosinophil peroxidase.

Table S3. Secondary antibodies used in immunofluorescence staining.

Antibody	Concentration	Clone ID	Reference	Source
IFKine™ Red donkey anti-rabbit IgG	1:100	polyclonal	A24421	Abbkine Scientific Company, Wuhan, China
IFKine™ Green donkey anti-mouse IgG	1:100	polyclonal	A24211	Abbkine
IFKine™ Red donkey anti-mouse IgG	1:100	polyclonal	A24411	Abbkine

Table S4. Lower detection limits for ELISA assay

Target	Detection limit	Manufacturer
25VD3	1.5 ng/mL	Ruixinbio, Quanzhou, China
1,25VD3	1.5 ng/mL	Ruixinbio
IL-36γ	18.75 pg/mL	NeoBioscience, Shenzhen, China
IL-5	7.8 pg/mL	Boster Biotechnology, Wuhan, China
IL-17A	31.3 pg/mL	Boster Biotechnology
IFN-γ	15.6 pg/mL	Boster Biotechnology

IL: interleukin; IFN: interferon

Table S5. Primers used for quantitative RT-PCR analysis.

Target	Primer sequence	Annealing temperature (°C)	Expect product size (bp)
VDR	(F)5′-TACGACCCCACCTACTCCG-3′	60	198
	(R)5′-ACTCAGATCCAGATTGGAGAAGC-3′		
CYP27B1	(F)5′-GGAACCCTGAACAACGTAGTC-3′	60	119
	(R)5′-AGTCCGAACTTGTAAAATTCCCC-3′		
CYP24A1	(F)5′-CGACTACCGCAAAGAAGGCTA-3′	60	218
	(R)5′-ACCATTTGTTCAGTTCGCTGT-3′		
IL36G	(F)5′-TAGGACCTCCACCCTTGAGTC-3′	60	76
	(R)5′-AATGATGGGCTGGTCTCTCTT-3′		
IL-5	(F)5′-CCCACAAGTGCATTGGTGAA -3′	56	81
	(R)5′-CCTCAGAGTCTCATTGGCTATCAG -3′		
IL-13	(F)5′-CCTCATGGCGCTTTTGTTGAC-3′	61	134
	(R)5′- TCTGGTTCTGGGTGATGTTGA-3′		
IL-17A	(F)5′-TCCCACGAAATCCAGGATGC-3′	62	75
	(R)5′- GGATGTTCAGGTTGACCATCAC-3′		
IFNG	(F)5′-TCAGCTCTGCATCGTTTTGG -3′	55	120
	(R)5′-GTTCCATTATCCGCTACATCTGAA -3′		
GUSB	(F)5′-GACACGCTAGAGCATGAGGG-3′	60	121
	(R)5′-GGGTGAGTGTGTTGTTGATGG-3′		

VDR, vitamin D receptor; CYP27B1, cytochrome P450 family 27 subfamily B member 1; IL, interleukin; IFN, interferon; GUSB, β-glucuronidase.

Table S6. Primary antibodies used in western blotting.

Antibody	Species	Concentration	Clone ID	Reference	Source
VDR	Rabbit	1:1000	polyclonal	GTX104615	GeneTex, Irvine, CA, USA
CYP27B1	Rabbit	1:1000	ERP20271	Ab206655	Abcam, Cambridge, UK
β-actin	Rabbit	1:1000	polyclonal	GB11001	Servicebio, Wuhan, China

VDR, vitamin D receptor; CYP27B1, cytochrome P450 family 27 subfamily B member 1.

Table S7. Antibodies used in flow cytometry.

Antigen-Fluorophore	Manufacturer	Clone ID	Source	Isotype	Dilution
CD45-BV421	Biolegend San Diego, CA, USA	HI30	Mouse	IgG1, κ	1:100
CD326-APC	Biolegend	9C4	Mouse	IgG2b, κ	1:100
VDR	Abcam, Cambridge, UK	polyclonal	Rabbit	IgG	1 μg/mL
CYP27B1	Abcam	ERP20271	Rabbit	IgG	1 μg/mL
Anti-rabbit IgG-FITC	Biolegend	polyclonal	Donkey	IgG(H+L)	1:200

VDR, vitamin D receptor; CYP27B1, cytochrome P450 family 27 subfamily B member 1.